

*Institute for Advanced Technology
The University of Texas at Austin*

Commissioning Tests of the Medium Caliber Railgun Launcher

*Keith A. Jamison
Institute for Advanced Technology
The University of Texas at Austin*

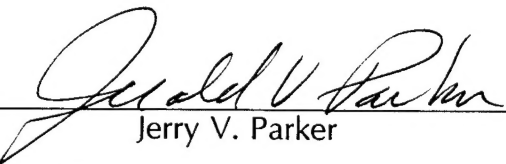
March 1996

19960621 027

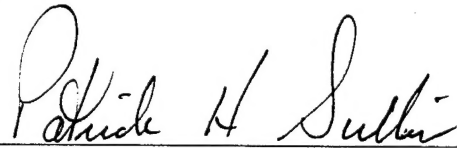
IAT.R 0101

Approved for public release; distribution unlimited.

Certificate of Technical Review



Jerry V. Parker



Patrick H. Sullivan

The views, opinions, and/or findings contained in this report are those of the author(s) and should not be construed as an official Department of the Army position, policy, or decision, unless so designated by other documentation.

REPORT DOCUMENTATION PAGE

Form Approved
OMB NO. 0704-0188

Public reporting burden for this collection of information is estimated to average 1 hour per response, including the time for reviewing instructions, searching existing data sources, gathering and maintaining the data needed, and completing and reviewing the collection of information. Send comments regarding this burden estimate or any other aspect of this collection of information, including suggestions for reducing this burden, to Washington Headquarters Services, Directorate for Information Operations and Reports, 1215 Jefferson Davis Highway, Suite 1204, Arlington, VA 22202-4302, and to the Office of Management and Budget, Paperwork Reduction Project (0704-0188), Washington, DC 20503.

1. AGENCY USE ONLY (Leave blank)	2. REPORT DATE	3. REPORT TYPE AND DATES COVERED	
	March 1996	Technical Report, Sept 1995 — Nov 1995	
4. TITLE AND SUBTITLE Commissioning Tests of the Medium Caliber Railgun Launcher			5. FUNDING NUMBERS Contract # DAAA21-93-C-0101
6. AUTHOR(S) Keith A. Jamison			
7. PERFORMING ORGANIZATION NAME(S) AND ADDRESS(ES) Institute for Advanced Technology The University of Texas at Austin 4030-2 W. Braker Lane, #200 Austin, TX 78759		8. PERFORMING ORGANIZATION REPORT NUMBER IAT.R 0101	
9. SPONSORING / MONITORING AGENCY NAME(S) AND ADDRESS(ES) U.S. Army Research Laboratory ATTN: AMSRL-WT-T Aberdeen Proving Ground, MD 21005-5066		10. SPONSORING / MONITORING AGENCY REPORT NUMBER	
11. SUPPLEMENTARY NOTES The view, opinions and/or findings contained in this report are those of the author(s) and should not be considered as an official Department of the Army position, policy, or decision, unless so designated by other documentation.			
12a. DISTRIBUTION / AVAILABILITY STATEMENT Approved for public release; distribution unlimited.		12b. DISTRIBUTION CODE A	
13. ABSTRACT (Maximum 200 words) Checkout tests and initial test firings of the IAT-HVL, seven meter long, 40 mm square-bore railgun were conducted in October 1995. This report details the initial performance of the Medium Caliber Launcher (MCL) and gives performance data for a simple "C" shaped solid armature. The commissioning tests include electrical data from tests with a fixed shorting block at the muzzle and very low energy tests for armature friction where the armature was either static or moved only part way down the barrel. The firing data consists of a six shot sequence devised to proof test the capacitor power supply, characterize the gun performance, and establish an armature behavior baseline set in terms of two critical issues, rail gouging and contact transition. Briefly, the power supply performed flawlessly, the railgun functioned well but with a slightly lower than expected inductance gradient, the onset of gouging was observed at 1350 m/s and the highest velocity observed before contact transition was 1970 m/s. The complete laboratory system of railgun, diagnostics, data acquisition, and pulsed power form a good test arena for the study of solid armature behavior.			
14. SUBJECT TERMS Armature; Commissioning Tests; Electric Gun; Electromagnetic Launcher; Railgun; Solid Armature		15. NUMBER OF PAGES 45	16. PRICE CODE
17. SECURITY CLASSIFICATION OF REPORT Unclassified	18. SECURITY CLASSIFICATION OF THIS PAGE Unclassified	19. SECURITY CLASSIFICATION OF ABSTRACT Unclassified	20. LIMITATION OF ABSTRACT UL

TABLE OF CONTENTS

Section	Title	Page
1.0	Introduction	1
2.0	Experimental Apparatus.	2
2.1	Railgun	3
2.2	Launch Package	3
2.3	Power Supply.....	4
2.4	Diagnostics.....	6
2.5	Data Acquisition System.....	7
2.6	Projectile Stop	7
3.0	Test Results	9
3.1	Shorted Muzzle	10
3.2	Static and Low Speed Armature Tests	15
3.3	Launch Experiments	16
3.3.1	MCL10 - First Launch, 8 kV Charge Voltage	17
3.3.2	MCL11 - 9.6 kV Extended Pulse Width.....	20
3.3.3	MCL12 - 12 kV Ripple Pulse; Plain Armature Contact.....	20
3.3.4	MCL13 - 12 kV Ripple Pulse; Laminated Armature	24
3.3.5	MCL14 - 12 kV Ripple Pulse; Grooved Faced Armature	26
3.3.6	MCL15 - 14 kV Ripple Pulse; Laminated Armature	28
4.0	Findings and Results.....	31
4.1	Inductance Gradient.....	31
4.2	Rail Gouging.....	35
4.3	Contact Transition.....	37
5.0	Conclusions.....	38
	References.....	39
	Acknowledgments.....	40
	Appendix A	41
	Distribution List	45

LIST OF FIGURES

Figure	Title	Page
2-1	Outline of 40 mm, 95 gram Check-Out Armature	4
2-2	Force versus Deflection Curves for 25 and 40 mm Armatures	5
2-3	Cross Section View of Projectile Stop	8
3-1	Inductance Gradient Computed from Measured Breech Voltage	12
3-2	B-dot Signal Compared to Time Rate of Change of Rail Current	13
3-3	Sensitivity of B-dot Probes as Computed from Measured Quantities	14
3-4	Shot Data for Test MCL10	18
3-5	Shot Data for Test MCL11	21
3-6	Shot Data for Test MCL12	23
3-7	Shot Data for Test MCL13	25
3-8	Shot Data for Test MCL14	27
3-9	Shot Data for Test MCL15	29
4-1	Muzzle Voltage versus In-Bore Armature Position for Three Shots	33
4-2	Muzzle Voltage, Velocity and Current versus Position for Test MCL15.	34
4-3	Location and Size of Rail Gouges	35
4-4	Gouge Length and Width	36
4-5	Velocity and Current at Each Gouge Location	36
4-6	Electrical Action versus Magnetic Pressure at Time of Transition	38

LIST OF TABLES

Table	Title	Page
3-1	Summary of Entire Test Series	9
3-2	Individual Module Resistances Determined from Shorting Block Tests ..	10
4-1	Inductance Gradient Needed to Match Simulations with Shot Data	32
4-2	Armature Transition Conditions	37

Commissioning Tests of the Medium Caliber Railgun Launcher

Keith A. Jamison

Abstract: Checkout tests and initial test firings of the IAT-HVL, seven meter long, 40 mm square-bore railgun were conducted in October 1995. This report details the initial performance of the Medium Caliber Launcher (MCL) and gives performance data for a simple "C" shaped solid armature. The commissioning tests include electrical data from tests with a fixed shorting block at the muzzle and very low energy tests for armature friction where the armature was either static or moved only part way down the barrel. The firing data consists of a six shot sequence devised to proof test the capacitor power supply, characterize the gun performance, and establish an armature behavior baseline set in terms of two critical issues, rail gouging and contact transition. Briefly, the power supply performed flawlessly, the railgun functioned well but with a slightly lower than expected inductance gradient, the onset of gouging was observed at 1350 m/s and the highest velocity observed before contact transition was 1970 m/s. The complete laboratory system of railgun, diagnostics, data acquisition, and pulsed power form a good test arena for the study of solid armature behavior.

1.0 Introduction

Railguns have been the subject of considerable research and development in the past 15 years. Although a variety of applications have been suggested as potential uses for railguns, the vision of a hypervelocity gun that can defeat future armored threats has been the most dominate. Seemingly countless mission studies have pointed out that the armature must be as efficient as possible in order to minimize the size of the pulsed power system needed to energize the railgun. In the laboratory, however, solid armatures are known to transition from a low voltage operating mode to a high voltage or arcing mode as velocities are increased.

Researchers also note gouging of the rails when aluminum armatures sliding on copper rails approach the velocity of conventional tank gun projectiles. Post shot inspections of laboratory railguns have also led most mission analysis studies to rank bore surface lifetime very high on the list of critical issues that must be addressed. Recognizing these two phenomena as perhaps the greatest concerns with present railgun technology, the IAT procured the Medium Caliber Launcher (MCL) as a test bed for armature/rail interaction research. In conjunction with this procurement a 13MJ, capacitor, pulsed power source was constructed in the south laboratory of the IAT Leander Research Complex using surplus equipment from the U.S. Army. These facilities now serve as the nation's primary laboratory for the study of solid armature behavior in railguns.

A short test plan for commissioning the railgun was written and reviewed prior to assembly and operation of the MCL. This test plan is given in Appendix A. Although the plan was not followed to the letter, the commissioning test series certainly followed the plan in spirit. Section 2 of this report documents the experimental hardware used in the initial test series. Section 3 describes all of the tests actually performed and Section 4 gives some results relating to the gun inductance gradient, rail gouging, and armature contact transition.

2.0 Experimental Apparatus

Railgun testing actually involves several systems including: a pulsed power supply, diagnostic probes, a data acquisition system, the launch package including the armature, and a projectile catch system. All of these systems must function with a certain degree of proficiency to accurately assess the performance of a railgun. As documented in this report, all of the hardware functioned well and a set of baseline performance data now exists for comparison to future experiments. Brief descriptions of each portion of the complete experimental apparatus is given in the following paragraphs.

2.1 Railgun

The launcher barrel consists of a pair of replaceable copper rails, 1.75" x 0.75", 25 feet in length. The rails are separated and backed by G-10 composite insulators to form a square 40 mm bore. The rails and insulators are held by a laminated steel containment designed to withstand the separating magnetic force that exists when an electrical current of 1.5 MA is flowing in opposite directions in each rail. The laminated containment pieces are positioned on a machined precision alignment surface that is supported by a large I beam. The I beam is supported and anchored to the concrete floor at several locations.

The rails are connected to the power supply by a large breech structure that has dual mating clamps to attach to both the inner and outer conductors of 40 large coaxial cables. Three of these large coaxial power cables are used to route current from each 1 MJ module of the power supply to the railgun.

2.2 Launch Package

The launch package consists of an aluminum armature and a polycarbonate fore body. Figure 2-1 shows an outline of the armature that was designed for the checkout tests. Initially, 21 armatures were wire electric discharge machined from 2 inch thick 7075 aluminum. The armature design was based on earlier work ^{1,2,3} on 25 mm railguns. The cross body of the armature is an arch, 0.4" thick with an insulator to insulator dimension of 1.555". This makes the available cross section for current conduction about 400 mm². The apparent contact area is about 3 times the cross body area, again scaled from previous successful armature designs. The trailing dimension of the armature is sized to be 0.04" (1 mm) larger than the bore while the leading dimension of the contact is only 0.002" larger than the rail to rail dimension. A forward key was included to serve as a dovetail connection to the fore body.

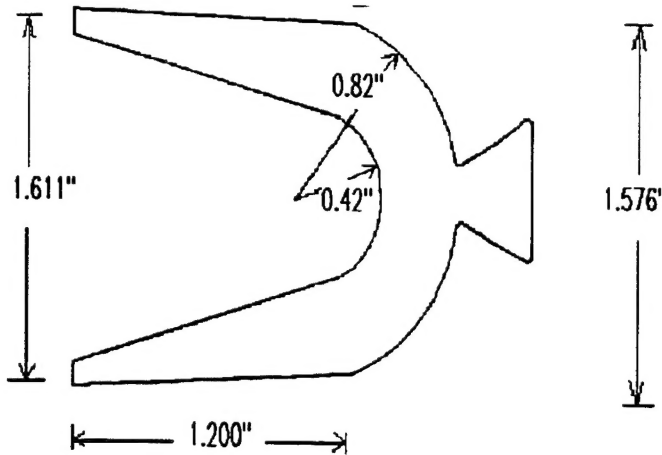


Figure 2-1. Outline of 40 mm, 95 gram Check-Out Armature

The compliance, or amount of force required to compress the armature to fit the actual bore dimension was designed to be in the range of 1000 to 2000 pounds. Compression tests with a precision vise and a load cell verified that the desired loading characteristics had been achieved.

Figure 2-2 shows the deflection of the largest armature dimension as a function of the applied force. As a consistency check, two armatures (labeled A and B), selected at random, were tested in an instrumented vise. Their behavior is nearly identical. Figure 2-2 also shows the compliance curves for a 25 mm armature for comparison. The major difference between the two armature sizes is that the 25 mm armature was 0.020" larger than the bore size while the 40 mm armature was 0.040" oversize. For the 40 mm armature one would anticipate the loading force to be about 350 pounds given a compression load of 1200 pounds and a static coefficient of friction in the neighborhood of 0.3. Although the force required to load the armature was not measured, several sharp blows from a shop hammer were required to move the armature into the loaded position.

2.3 Power Supply

The capacitor power supply⁴⁾ for the railgun is comprised of ten, one-megajoule modules. Each module can be modeled as a series capacitor and

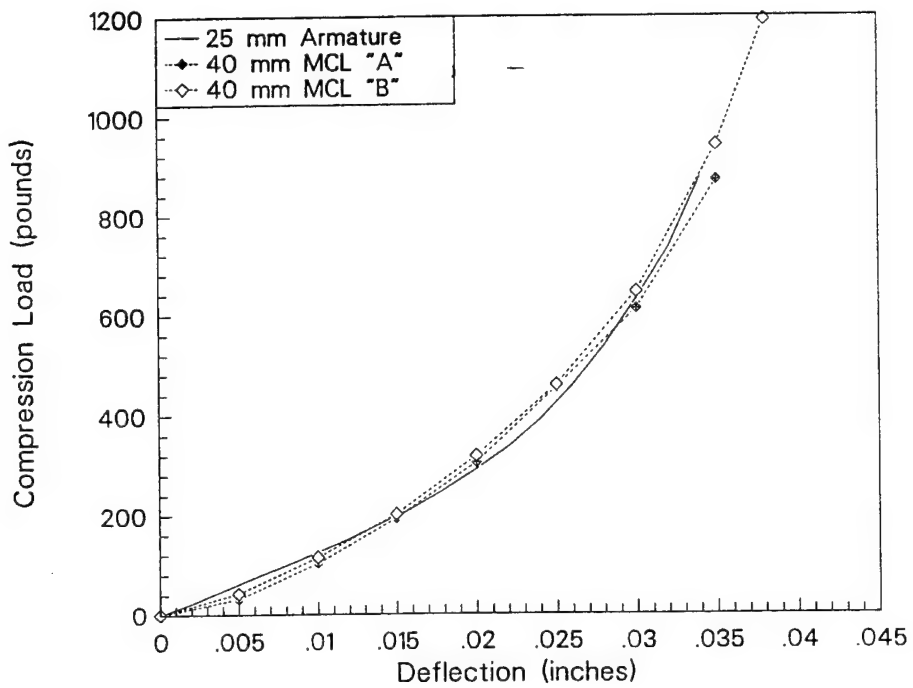


Figure 2-2. Force versus Deflection Curves for 25 and 40 mm Armatures

inductor with two switches, one to connect the module to the load and the other to short out the capacitor during the discharge cycle to prevent voltage reversal (crowbar). Each module is connected to the railgun breech by three coaxial cables with the only common point being the massive plates that comprise the breech of the railgun. All modules may be independently triggered in a time sequence to produce a variety of current waveforms. For simple modeling the capacitance of a module is taken as 4.5 millifarads and the inductance as 26 microhenries. The last three modules (designated as banks #11, #12, and #13 in the facility) have different ignitron switch gear than the first seven modules (designated as banks #4 - #10 of the facility). For the first seven modules (#4 - #10) adequate simulations may be achieved by using a resistance of 11.5 milliohms before the crowbar circuit is activated and 10 milliohms after the crowbar ignitrons have been switched on. The last three modules have extra resistance in the crowbar circuit. Values of 6 and 23 milliohms proved to be adequate for the resistance before and after crowbar, respectively. The parameters discussed above were obtained by matching simulation code output to measured currents. As such, the reader is cautioned that any error in the calibration of the current probes will result in an error in the

module circuit parameters given here. Since the capacitance is derived from the manufacture's specifications and the inductance strongly influences the pulse width, the only terms with a significant uncertainty are the module resistances. Also note that, although the lengths of the coaxial connections from each module to the breech differ significantly, no significant differences in current were noted between modules other than those discussed above.

2.4 Diagnostics

Three types of diagnostic probes were used in this test series. They include: ten capacitor bank Rogowski coils, 14 rail B-dot sensors, and two isolated voltage dividers for the breech and muzzle of the railgun. The Rogowski coils were designed, fabricated, and calibrated in house. They are mounted on the output bus of the each module where current is fed to the coaxial connectors. The signals are routed to the breech area of the railgun by coaxial signal cable inside individual runs of soft copper tubing for added shielding. All data signals are routed from the breech patch panel to the control room in a grounded cable tray. All ten Rogowski coils have sensitivities within two percent of 6.6×10^7 A/Vs. In practice, all of the coil signals were recorded separately and multiplied by their individual scale factors before any further data analysis.

The B-dot sensors were supplied by the gun manufacture. At each axial measurement position there were two coils, one located above the center line of the positive rail and the other above the negative rail. These coils may be used separately or they may be connected in series so that the signal amplitudes add when current is flowing in opposite directions in the rail pair. Adequate simulation of the probes was achieved by modeling each sensor as a four turn loop with an area of 3.5 mm^2 , located 2 cm from a thin conductor carrying the entire railgun current. The probes are constructed on circuit board material cut in a shape to exactly match the laminates of the containment structure. The probes are placed between laminate sections on the top of the gun as it is assembled. The first laminate section beginning at the breech is about eight and a half inches long making the first B-dot location 21.1 cm. Subsequent laminate sections are about

20 inches in length so that the typical B-dot spacing is 52 cm. In practice the actual locations of the probes were measured after the gun was assembled so that a probe location accuracy of better than 1 mm could be provided to the data analysis codes.

Isolated, voltage probes for the breech and muzzle of the launcher were also fabricated in-house. They consisted of a resistive link between the two points of interest with the link passing through a current-to-voltage conversion transformer. Calibration was accomplished simply by measuring the resistance of the resistive link and using the manufacture's specifications for the current transformer. The sensitivity of the breech probe was 1007 V/V and 136 V/V for the muzzle voltage probe.

2.5 Data Acquisition System

A computer controlled, digital recording system manufactured by LeCroy was the heart of the data acquisition system. The system is comprised of four CAMAC crates each holding four LeCroy 6810 four channel digitizers so that up to 64 probes may be monitored. For this work 26 channels of data were collected on each shot. Each signal record was 8,000 samples in length, typically, recorded at a 1 MHz sampling rate. Simulations were run before each test to estimate the anticipated amplitude of each probe's signal. The sensitivity of each input amplifier was set to match the expected signal. After each test the data was archived on a PC hard drive then converted and copied to floppy disks for analysis by different software packages.

2.6 Projectile Stop

It is often useful to recover portions of the launch package for post shot inspection. This is easily accomplished with small bore (low energy output) railguns by firing into a large container of soft material such as cloth rags. As projectile energy increases, the task of stopping a launch package without significant damage becomes much more difficult. To facilitate recovery of higher energy launch packages a crude soft catch system was constructed using the containment struc-

ture of a previous railgun and Homosote, a pressed paper building supply board available in half inch thick 4 x 8' sheets. Two, 2 meter sections of the steel containment structure were positioned down range from the railgun and centered on the shot line with the alignment telescope. Strips of building material were cut to fill the containment leaving an open channel slightly smaller than the launch package dimensions as shown in Figure 2-3. The strips were actually cut to significantly over fill the containment structure so that when the top and bottom containment sections were bolted together the homosote was compressed.

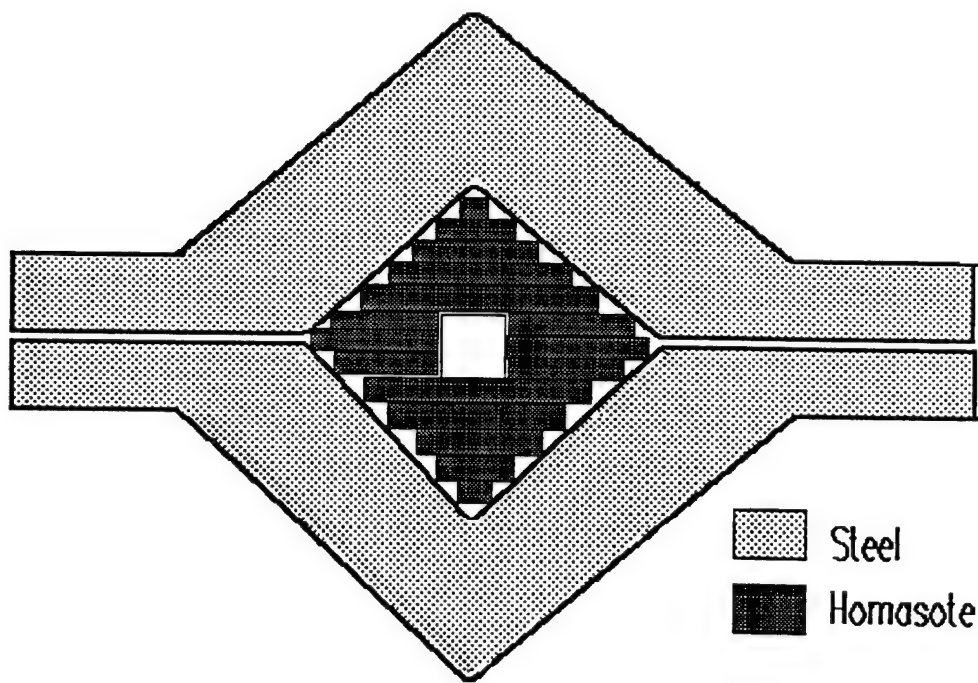


Figure 2-3 Cross Section View of Projectile Stop

Results with the soft catch system were mixed. In all cases pieces of armatures were recovered but only one high energy armature was recovered as a single piece. If a stronger fore body were used with future armature tests the likelihood of armature recovery would be increased.

3.0 Test Results

In all, current was applied to the railgun for fifteen tests. Three tests used a shorting block at the muzzle, five shots had a static or very slowly moving armatures, six were actual projectile launches and one was an unrecorded prefire of an ignitron during charging. Table 3-1 summarizes the entire test series.

Table 3-1 Summary of Entire Test Series

Folder	Date	ID	Opera-tions Log	Charge Voltage (kV)	Bank #'s	Max. Current (kA)	Mass grams	Notes
MCL01	6 Oct. 95	95100603	137	5	4,6,7		-	Muzzle Short
MCL02	9 Oct. 95	95100901	138	5.07	4,5,6	148	-	Muzzle Short
MCL03	9 Oct. 95	95100902	139	5.07	11,12,13	157	-	Muzzle Short
MCL04	12 Oct. 95	95101203	142	6	5		173.9	Static armature
MCL05	12 Oct. 95	95101204	143	7	4,5,6		same	Moved 16 "
MCL06	12 Oct. 95	95101205	144	8.5	4,5,6	none	same	Non-Shot
MCL07	13 Oct. 95	95101301	145	9.09	7,8,9	307	same	Moved 1 meter
MCL08	13 Oct. 95	95101302	146	9.61	7,8,9,10	424	same	Moved 4 meters
MCL09	13 Oct. 95	95101303	147	7.6	7,8,9,10	288	same	Armature Exit
MCL10	16 Oct. 95	95101601	148	8.12	all	939	174.8	950m/s
MCL11	17 Oct. 95	95101702	150	9.62	all, 1 delayed	1003	168.4	Plain armature
MCL12	19 Oct. 95	95101902	152	12	all, four ripple fired	837	164.93	Plain armature
MCL13	23 Oct. 95	95102301	153	12	all, four ripple fired	838	170.96	Laminated armature
MCL14	24 Oct. 95	95102401	154	12	all, four ripple fired	834	168.2	Grooved face armature
MCL15	25 Oct. 95	95102501	155	14	all, four ripple fired	997	171.24	Laminated armature

In Table 3-1 the tests are cross referenced to the operations log of the power supply and to the test designation used in archiving the data (the column labeled "ID").

3.1 Shorted Muzzle

To determine the electrical characteristics of the railgun and power supply a robust shorting block was fabricated to fit tightly in the bore at the muzzle of the gun with a screw wedge arrangement. Three tests were performed. The first discharge was a test to verify that signals were observed on all diagnostic lines. The second and third tests were performed for three reasons: a) to obtain current traces so that the simulation codes could be anchored to actual performance data, b) to obtain an estimate of the railgun inductance by observing the breech voltage, and c) to determine the sensitivity of the B-dot probes. Since the power supply consists of modules constructed with two different configurations two tests were performed. Test MCL02 used modules #4, #5, & #6 while test MCL03 used modules #11, #12, & #13. The observed current traces were compared to simulation runs with different bank resistance parameters. The simulated peak current is quite sensitive to the power supply's resistance before the crow bar circuit is activated. The current decay rate after its peak is somewhat sensitive to the simulated circuit resistance after the crowbar is switched on. The simple code used for these simulations does not allow for time varying circuit parameters in the power supply. However, reasonable match to the data was achieved after comparing numerous simulation runs to the observed data. The results are given below in Table 3-2.

Table 3-2 Individual Module Resistances Determined from Shorting Block Tests

Test / Modules	Resistance Before Crowbar (milliohms)	Resistance After Crowbar (milliohms)
MCL02 #4, #5, & #6	11.5	10.0
MCL03 #11, #12, & #13	6.0	23.0

Railguns are usually constructed so that their dominate electrical impedance is inductive. The use of massive copper rails keeps the resistance low and helps to make the gun efficient. The MCL is no exception to this generality. As such, the voltage that appears on the breech when a current pulse is directed through a muzzle shorting block is primarily due to the gun inductance, and given by

$$V = L \frac{di}{dt} - iR(t) \quad (1)$$

where L and R are the inductance and resistance of the rails, respectively. The inductance gradient, L' can be written as

$$L' = \frac{V_{breech} - iR(t)}{l \frac{di}{dt}} \quad (2)$$

where l is the length of the gun and V_{breech} , di/dt , and i are all measured quantities. Since $R(t)$ is not a dominate term it may be approximated by a skin depth type function that varies inversely with the square root of time. The overall scaling of value of $R(t)$ may be adjusted to obtain the correct voltage at peak current where $di/dt = 0$. Data from test MCL03 was compressed and loaded into a spreadsheet where Equation (2) was solved for L' . The results, shown in Figure 3-1, were not anticipated. Experience with other railgun measurements shows a low inductance gradient at very early times rising to a larger, constant level as time increases. This is the expected behavior based on the current diffusion effect. Current initially flows on the inner rail surfaces which minimizes the volume of magnetic field. Later, as the magnetic field and current diffuse into the rails, the area of the current loop is increased, thereby increasing the inductance. The observation of a large inductance gradient at early time is inconsistent with this picture.

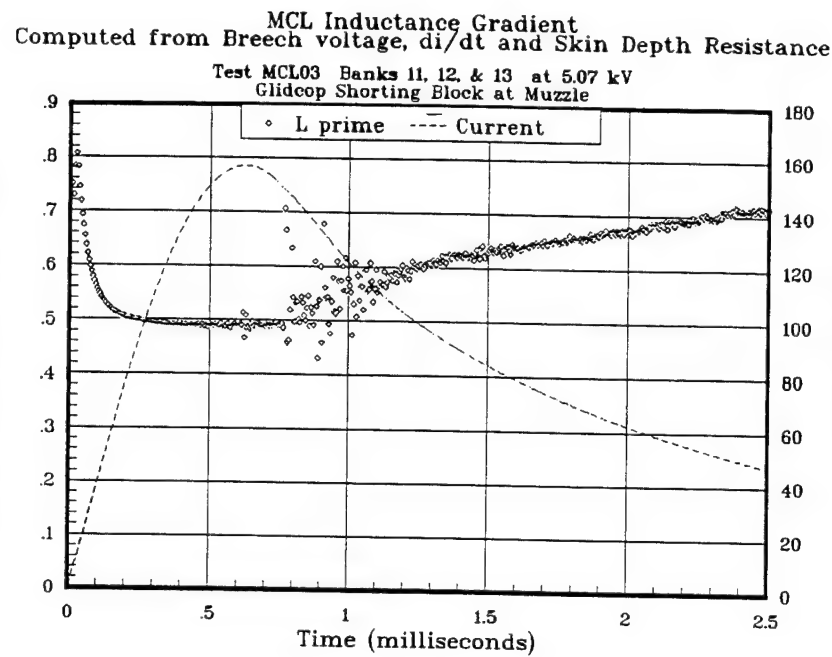


Figure 3-1 Inductance Gradient Computed from Measured Breech Voltage

A further concern with this analysis is that the level portion of the calculation (between 200 and 800 microseconds) is 0.48 microhenries per meter rather than 0.44 microhenries per meter calculated for a 2-D vacuum field with perfectly conducting rails. Although no adequate explanation for this result has been found, two factors must be considered. First, the stainless steel containment is quite close to the rail pair in this launcher design and a complicated eddy current flow pattern surely exists for millisecond time-scale pulses in the rails. Eddy currents tend to lower the observed inductance so this would not account for the high values in this analysis. Second, the stainless steel containment is weakly ferromagnetic and may be acting as a magnetic core, at least at low current levels where the fields are not strong. This would have the effect of increasing the observed inductance so it remains a possibility. Further analysis and experimentation are needed to clarify this issue.

When the rail pair is shorted at the muzzle, current in the rails flows past all 14 B-dot probes. The changing magnitude of current produces a changing magnetic field that is sensed by the B-dot probes even though no mechanical motion is occurring in the system. In free space, the voltage induced on each B-dot loop

will be exactly proportional to the time rate of change of the current with the proportionality constant being only a function of the location, orientation, and size of the current and probe loops. Prior to this test it was anticipated that the sensitivity of the probes would be on the order of 1.3×10^9 A/Vs, based on very simple approximations of the magnetic field near a current carrying conductor. It was also anticipated that the B-dot signatures would exactly match the measured functional form of time rate of change of current in the rails.

After test MCL03 (a three module discharge with the muzzle shorted) the signals from the Rogowski coils on all three modules were summed and compared to the signals from each of the B-dot probes. Although all 14 of the B-dot signatures were remarkably similar in both form and amplitude, there was notable difference between the time rate of change of current and the B-dot signals. Figure 3-2 illustrates this difference by plotting the di/dt signal from the rail current along with the average signal from the 14 B-dot probes.

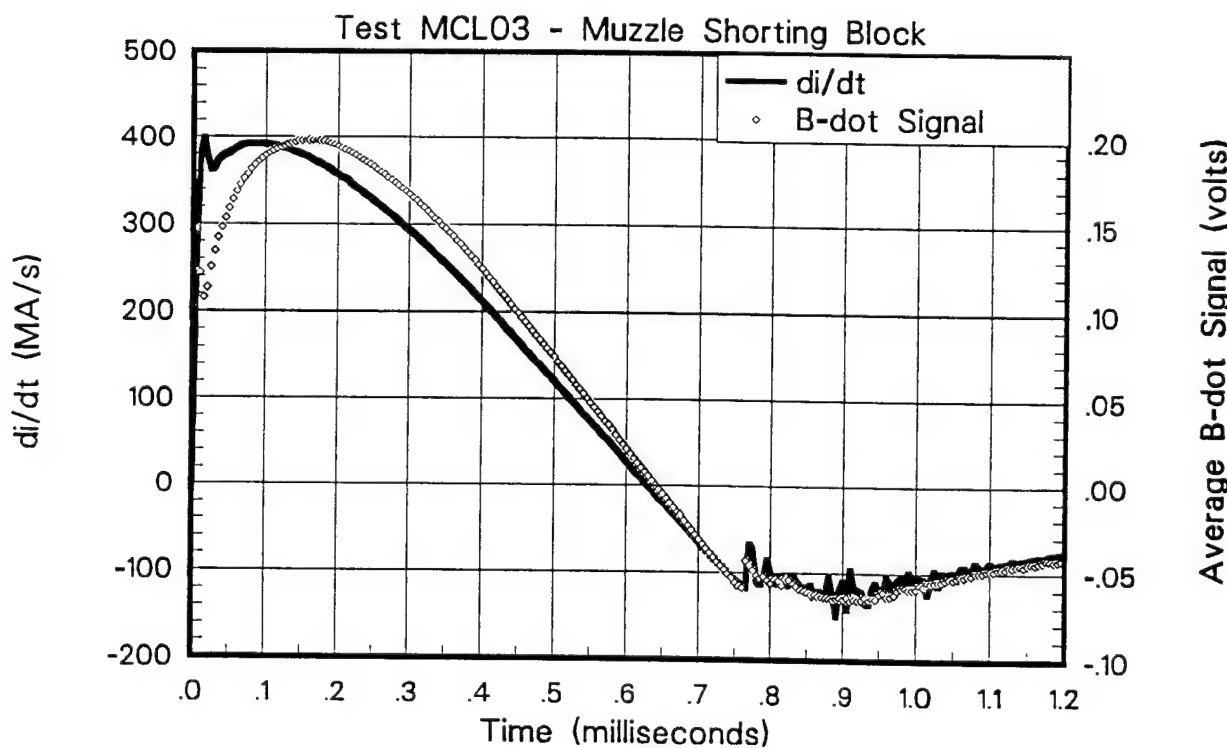


Figure 3-2 B-dot Signal Compared to Time Rate of Change of Rail Current.

Although both traces in Figure 3-2 have approximately the same functional form, they are clearly not related by a simple proportionality constant. The B-dot signal is suppressed by nearly a factor of two at early times and appears to lag the di/dt trace at later times. The difference is even more pronounced if one attempts to compute a calibration constant, or scale factor for the B-dot probes by dividing the time rate of change of current by the observed B-dot signal. Figure 3-3 illustrates this point by displaying the ratio of the two quantities as a function of time for the first 2.3 milliseconds of the discharge. It is noted that both quantities were near zero around 0.62 milliseconds so the ratio should be ignored near that time.

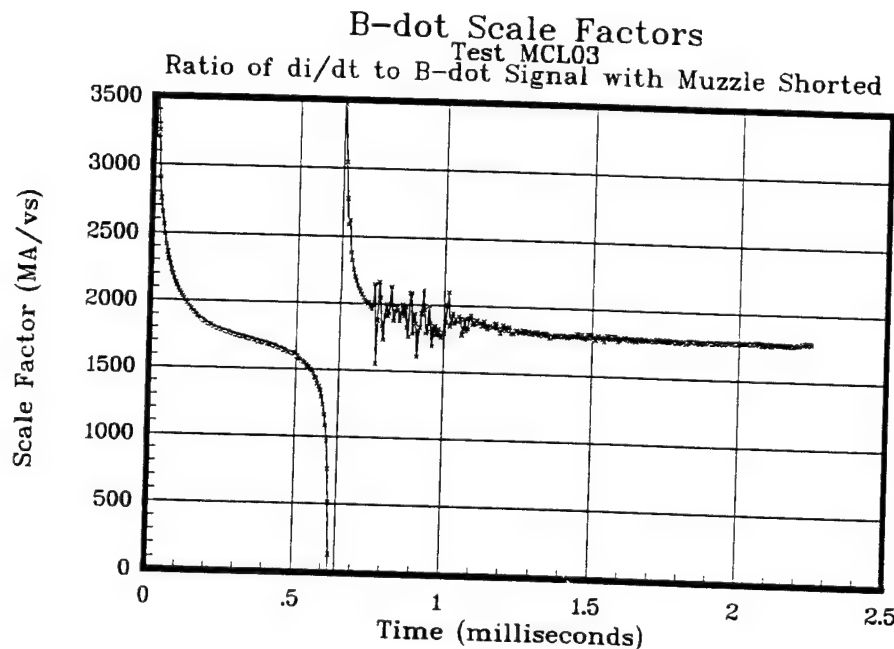


Figure 3-3 Sensitivity of B-dot Probes as Computed from Measured Quantities

As with the discussion of the inductance gradient given above, the B-dot probes may be subject to eddy currents in the containment and support structure. The ferromagnetic effects of the steel containment may also be important. Again, the result is reported here without conclusion. The sensitivity of the B-dot probes may be taken as 1.7×10^9 A/Vs given the caution that time dependent effects most certainly exist.

3.2 Static and Low Speed Armature Tests

Several tests were performed with an armature and fore body inserted in the railgun prior to attempting a projectile launch. An armature and polycarbonate fore body were loaded in the railgun with the center of the armature cross bar 0.15 m (6 inches) in front of the forward most surface of the breech connecting plate. This location was chosen to meet the so called “four caliber rule” that states that 95% of the full accelerating force exerted on an armature results from the magnetic field associated with current flowing in the rails within four bore heights of the armature. This distance is also chosen to avoid perturbing influences from currents in the breech current connections.

The purpose of the static tests were two-fold. First, some of the armature electrical characteristics may be determined from the measured muzzle voltage. Second, the resistance and inductance of the breech connection may be found from the breech voltage. Again, the electrical characteristics are dynamic quantities but comparison of measurements to simulations, even with fixed, zero-dimensional electrical quantities, is often useful. The railgun was pulsed with current from a single module charged to 6 kV for test MCL04. Using the measured current waveform a suitable match to the observed muzzle voltage was obtained using armature circuit parameters of 5 nanohenries and 10 microhms. The breech voltage computation suffers from the difficulties discussed in the previous section but an inductance of 30 nanohenries and a resistance on the order of 10 microhms gave a reasonable match between simulation and data. While these values do not have high accuracy they are useful first estimates for beginning a test series.

With the armature tightly placed in the railgun it appeared prudent to simply discharge the power supply at a higher level and clear the bore in an actual shot. A low exit velocity was desired because the down range projectile stop had not been completed at this point. However, the frictional drag force on the armature was completely unknown. There are unpublished reports that friction on monolithic aluminum armatures is quite small once acceleration begins. This led to

a conservative choice of input power for Test MCL05, three modules charged to 7 kV. The discharge was exactly as planned but the armature moved only 16 inches. Owing to the rather short distance traveled friction could not be estimated accurately so the test was repeated with a charge voltage of 9 kV for test MCL07. Again, minimal motion of the armature was noted, (the armature moved about one meter) stopping about 1.5 meters from the breech. For test MCL08 the input energy was increased again by selecting four modules and increasing the charge voltage to 9.6 kV. These parameters were selected because the simulation code, modified to include a constant frictional drag force of 350 pounds, indicated that the projectile would just exit the bore before the velocity was reduced to zero. During test MCL08 a peak current of nearly 400 kA was delivered to the gun and B-dot sensors gave the anticipated signals as the armature passed six probes before coming to rest 0.75 meters from the muzzle of the gun. At low speeds (200 m/s or less) friction is apparent and strong enough to stop an armature in a long railgun. A final test, MCL09, was used to clear the armature from the barrel. Some deposits of aluminum were evident on the rails from the six tests conducted with the first armature. In preparation for the first launch experiment a sanding block was fabricated and used to lightly sand the rail and insulator surfaces. After sanding, the bore was cleaned by pushing bundles of cloth rags through the barrel.

3.3 Launch Experiments

The test plan given in Appendix A called for starting the test series at a fairly significant current level and then increasing the peak current gradually while, at the same time, increasing the width of the current pulse. The result would be a rather aggressive step up in launch package kinetic energy for each test. The conditions for the first test were chosen to achieve a velocity of almost 1 km/s. For all subsequent tests the results of the previous test were reviewed and discussed before proceeding.

3.3.1 MCL10 - First Launch, 8 kV Charge Voltage

The simulation code, adjusted to match the data obtained from the previous tests, was run to select the bank discharge parameters for the first launch by the MCL. The code indicated that all ten modules, charged to 8 kV would produce a current slightly over 900 kA and a projectile velocity in excess of 1 km/s for a 175 gram mass launch package.

The armature was loaded 6 inches in front of the breech connection and all ten modules were charged to 8.12 kV. The resulting electrical current produced results that were very much as expected with two exceptions, the in-bore acceleration time was longer than predicted and the muzzle voltage showed numerous transitions from a few volts to levels of 20 to 40 volts. A peak current of 939 kA was recorded and all 14 B-dot probes clearly tracked the trajectory of the armature down the barrel for 8 milliseconds. The in-bore velocity, as derived from B-dot signatures, reached about 1 km/s between B-dot probes 6 and 7. The exit velocity was somewhat slower, on the order of 900 m/s. Simulation code, including the previously observed friction and an inductance gradient of 0.44 microhenries per meter, predicted an exit velocity of 1.08 km/s with a total in-bore time of 7.13 milliseconds. To match the exit time of the armature the inductance gradient in the simulation code had to be reduced to 0.365 microhenries per meter. This is well below the value indicated by the static electrical tests and the Kerrisk value for perfectly conducting rails.

All of the shot data for the six firing are displayed in a similar fashion to the data from test MCL10 that are presented in Figure 3-4. In addition to the current and muzzle voltage, the breech voltage, time rate of change of current (di/dt), the actual B-dot probe signals and some simulation results are shown. In all cases the data has been compressed to a slower time base than the acquisition rate for easier graphing. In the upper right graph of Figure 3-4 are the simulation results when the inductance gradient is reduced to 0.365 microhenries per meter to match the simulated and actual exit times. The times of the B-dot signal peak amplitudes

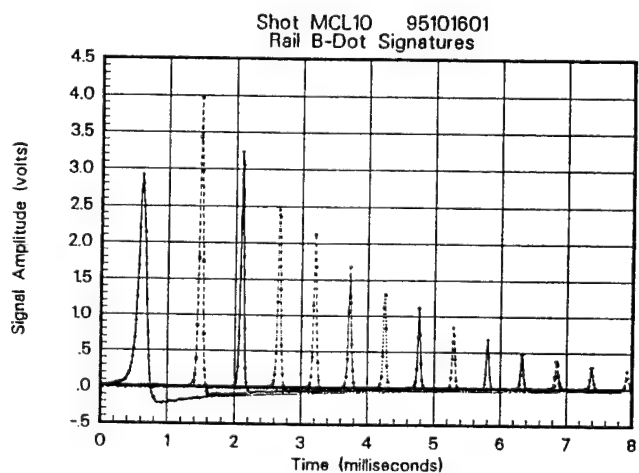
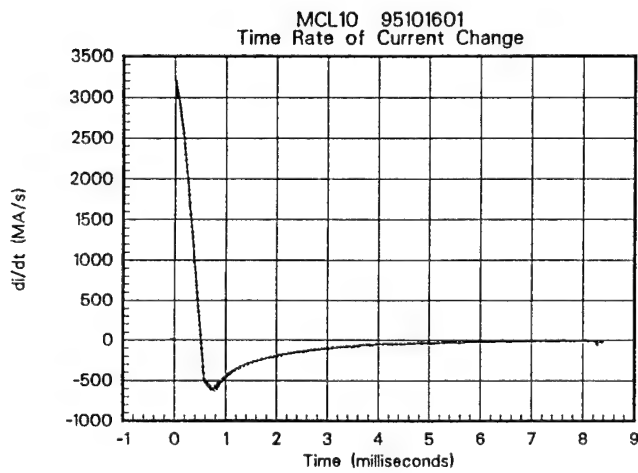
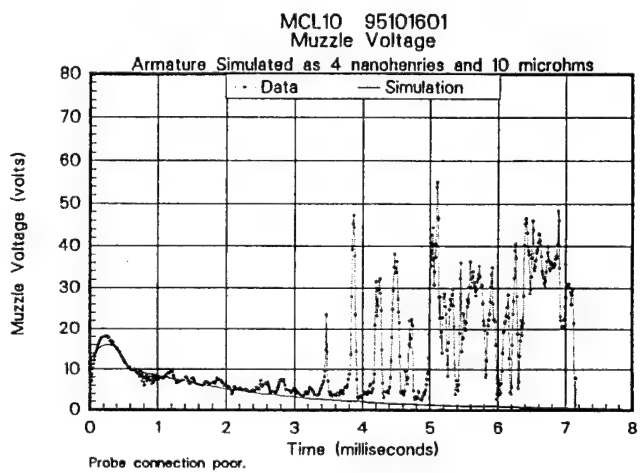
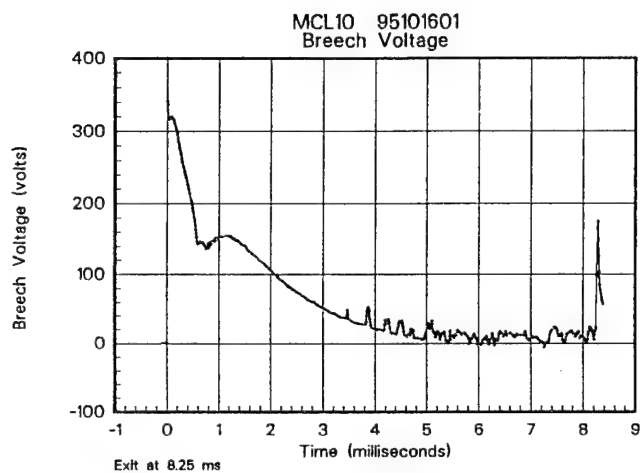
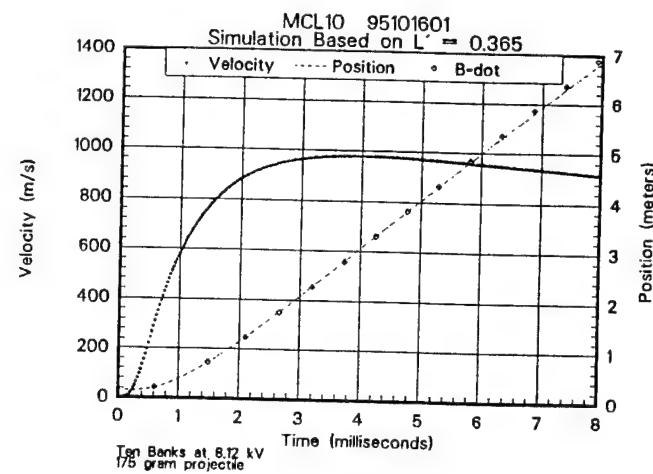
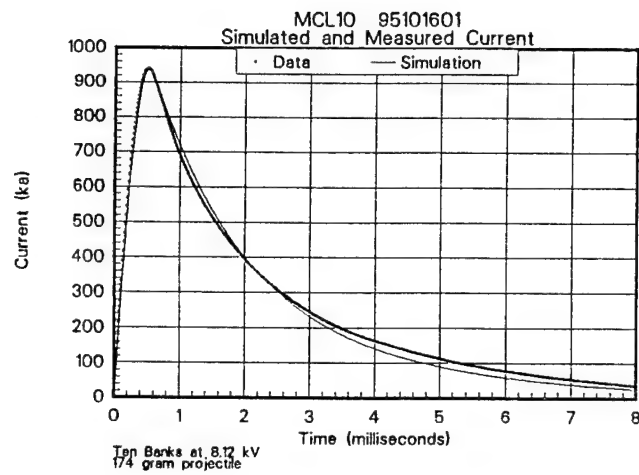


Figure 3-4 Shot Data for Test MCL10

are plotted versus the location of each probe to compare with the simulated position versus time history. Other shot data from MCL10 in Figure 3-4 includes the breech voltage, time rate of change of current, and a composite plot of all 14 B-dot probe signals. Of particular interest is the muzzle voltage, shown in the center plot on the right hand side of Figure 3-4. The voltage rises to about 18 volts in the early portion of the trace. This is consistent with a circuit element that has both resistive and inductive components. An approximate match to the early portion of the muzzle voltage waveform can be achieved by modeling the armature as a series combination of 4 nanohenries with 10 microhms. Although there are some small (2-3 volt) deviations from the simulated muzzle voltage the armature appears to have functioned with good solid contact for the first 3.5 milliseconds. After 3.5 milliseconds, numerous excursions of 10 - 30 volts are evident. This would indicate that one or both of the armature contacts are not functioning as efficiently as possible. The muzzle voltage signal does not, however, exceed 50 volts suggesting that a plasma armature did not form. The B-dot probe signals also remain compact well past 3.5 milliseconds, more characteristic of a solid rather than a plasma armature.

The first evidence of armature transition occurred at a velocity of about 1 km/s after the armature had incurred an electrical action of only $1.0 \times 10^9 \text{ A}^2\text{s}$. Both values are far below the design goals for the armature. At the time of transition, 3.47 milliseconds, the current had fallen below 200 kA. The "C" shaped armature depends on magnetic forces to develop pressure on the contacts in order to maintain low voltage operation. Premature transition is not unexpected given the greatly reduced magnetic pressure late in the current pulse.

The recovered armature showed considerable evidence of melting on the contact faces but had lost only 2 grams in mass. Inspection of the bore showed deposited aluminum but gave no indication that any problems existed with the railgun at the point of transition so the decision was made to proceed with the next shot at a higher current level. The test plan also called for extending the pulse

width of the current by delaying the firing of one bank. Both changes would tend to increase the magnetic pressure on the contacts at higher velocities. After the bore inspection, the bore was cleaned with a sanding block and wiped with cloth rags for the next shot.

3.3.2 MCL11 - 9.5 kV Extended Pulse Width

To achieve a higher peak current while delaying the firing of one module requires a substantially higher charge voltage. For test MCL11 the modules were charged to 9.6 kV, storing 40 percent more energy than the previous test. The firing signal for Bank #14 was delayed by 540 microseconds with respect to all other modules. The capacitor discharge produced a current in excess of one million amperes and the in-bore acceleration time was reduced to 6.3 milliseconds. The launch package achieved an in-bore velocity of 1.4 km/s, accumulating more than 150 kJ of kinetic energy. Shot data for MCL11 are shown in Figure 3-5. The graphs are arranged to match the previous test for quick comparisons. The current pulse width has broadened due to the delayed firing of the last module. The breech voltage is considerably larger in the region around 1 millisecond because of the increased speed voltage and the extended current pulse width. The muzzle voltage trace shows a transition at 2.3 milliseconds when the velocity was 1.27 km/s. Although the armature was still not being pushed to its full designed performance limits this was clearly an improvement in armature performance from the previous test. The B-dot signals increased in amplitude and their spacing in time decreased from the higher velocity. The condition of the bore, however, was far from pristine so the rails were removed and the insulators cleaned before the barrel was reassembled for the next test.

3.3.3 MCL12 - 12 kV Ripple Pulse; Plain Armature Contact

The measurement of the bore of the newly assembled barrel indicated that the rail to rail spacing was slightly smaller than anticipated. Both armature faces

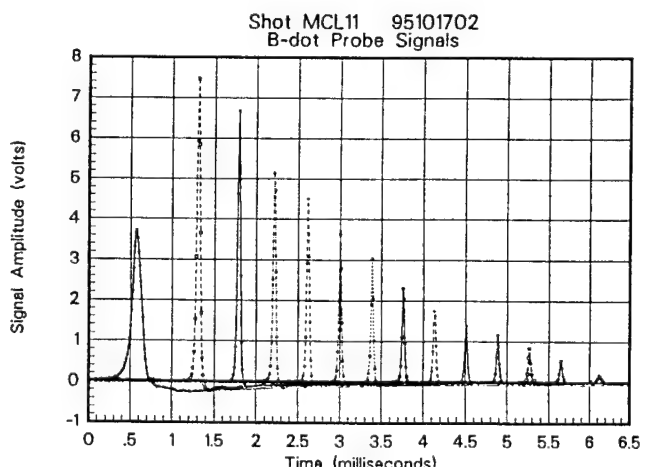
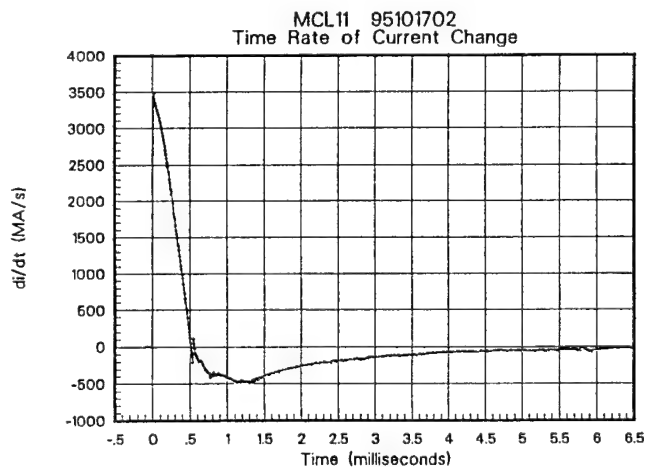
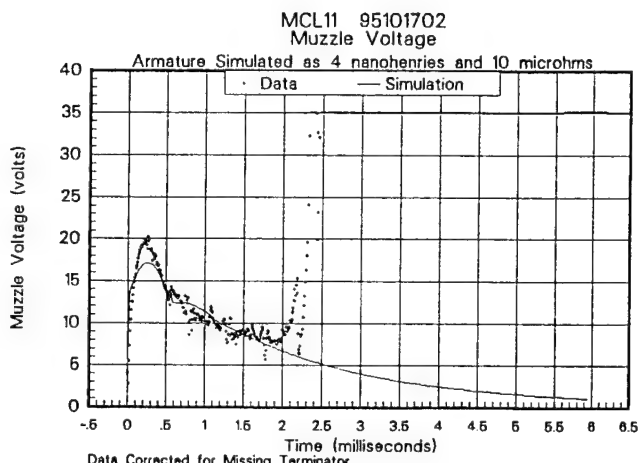
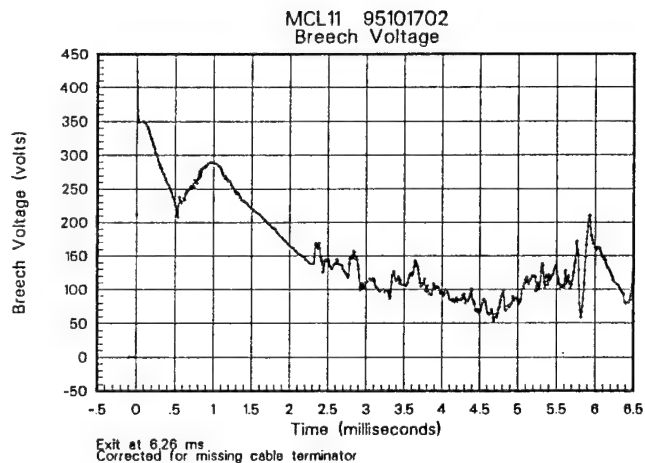
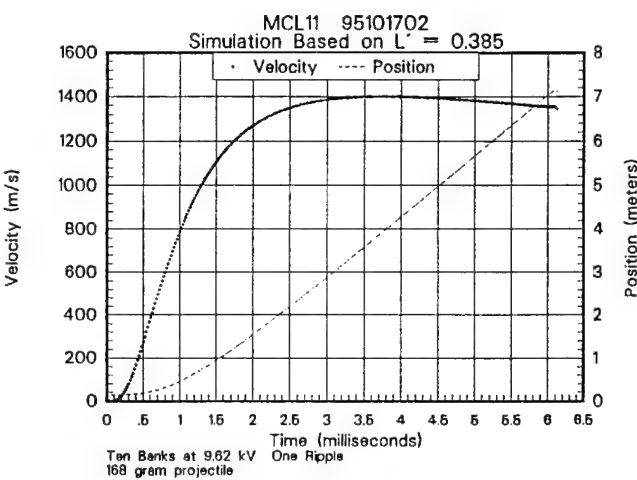
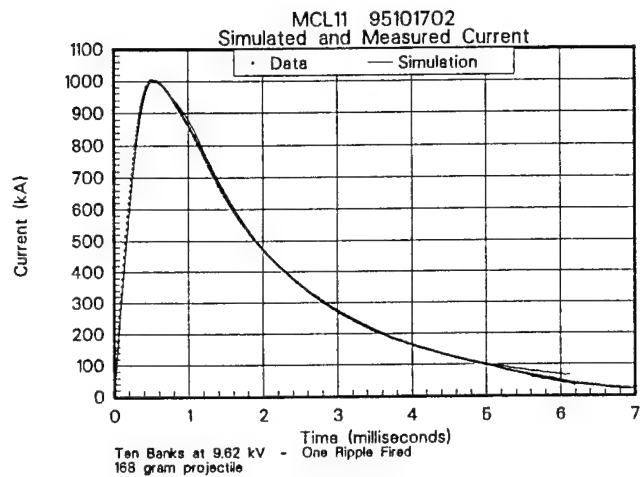


Figure 3-5 Shot Data for Test MCL11

were machined on a mill to remove 0.002" to accommodate this change. This reduction still left the forward portion of the armature slightly larger than the bore dimension so that the entire contact surface would be in contact with the rail when the launch package was loaded.

The apparent success in improving armature performance by extending the pulse width led to a decision to attempt a greatly extended current pulse width. A test with six modules fired initially followed by four delayed module firings had been planned for the last shot in the test sequence. Simulations were run to find the delay times that would produce a flat topped current pulse with a charge voltage of 12 kV. The simulations indicated that delay times of 580, 1000, 1400, and 1700 microseconds would yield a nearly flat current pulse for about 2 ms with an amplitude in excess of 800 kA. The simulations also indicated an increase of projectile kinetic energy of 65% over the previous test. The simulation results and the shot data for Test MCL12 are given in Figure 3-6. As shown in the upper left of Figure 3-6 the observed current trace is a very close match to the simulation. The ripple firing of the modules created the easily recognizable saw tooth pattern in the di/dt trace and matching steps in the breech voltage. The breech voltage climbed to 650 volts just as the last module began its discharge. As evidenced by the timing between B-dot probes the velocity reached 1.8 km/s and was a fair match to the simulation. The muzzle voltage indicated good armature contact performance for nearly 2.4 milliseconds at which time the velocity was over 1.5 km/s. Again, small oscillations appeared in the muzzle voltage trace before transition but generally the armature is well modeled as a simple circuit element with a 4 nanohenry inductance and a 10 microhm resistance. The muzzle voltage trace in Figure 3-6 includes the voltage expected from such a circuit element for comparison.

After the test, inspection of the bore showed strong aluminum deposition at the breech end, heavy black soot at the muzzle end and evidence of gouging about 2 meters down the bore. The barrel was disassembled for more detailed inspection

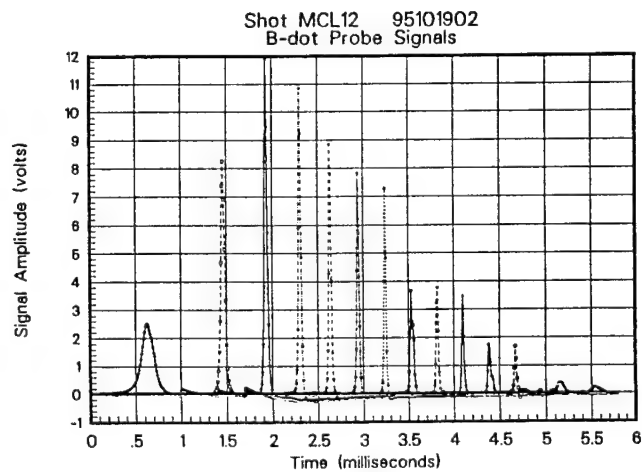
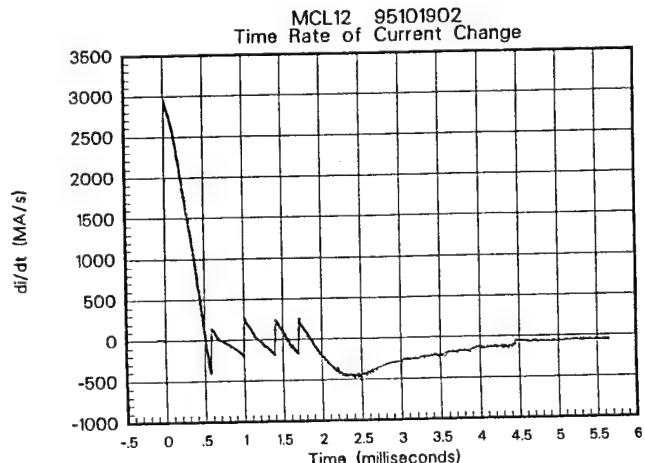
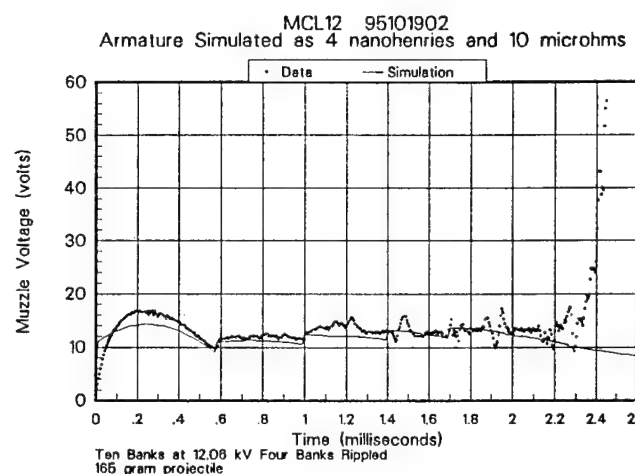
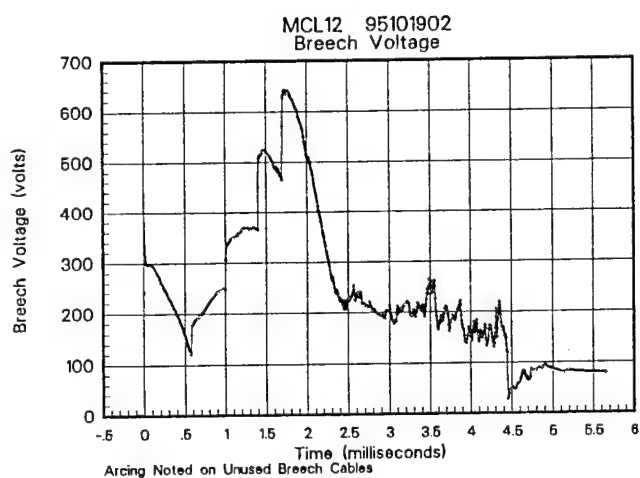
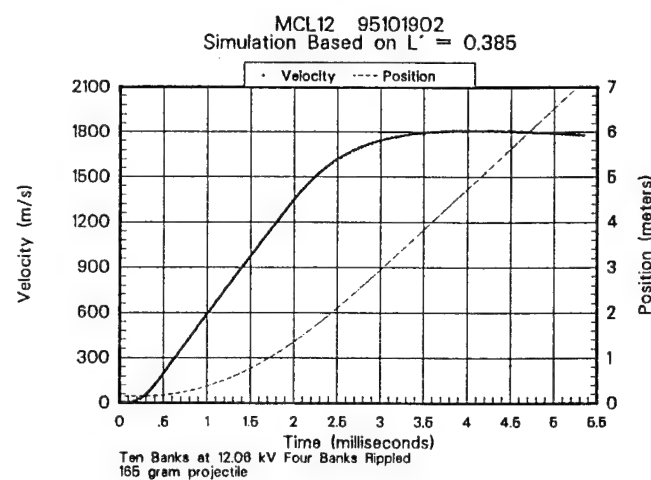
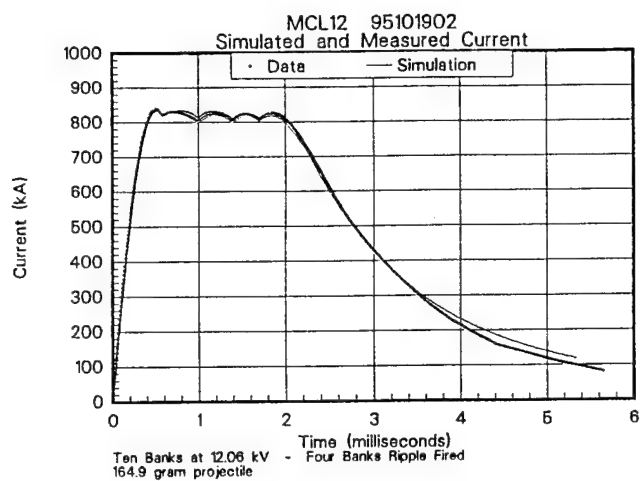


Figure 3-6 Shot Data for Test MCL12

of the rails. The first gouge appeared at a location 1.4 meters from the breech where the velocity was estimated to be 1.35 km/s. Several more gouges were noted before the transition point at 1.7 meters and a few more were found as far down the bore as 3 meters. After the three meter point heavy soot indicated that the armature was probably acting as a hybrid with plasma brushes connecting both contact faces to the rails.

Test MCL12 was highly successful in establishing bench marks for two important phenomena, contact transition and high velocity rail gouging. From these bench marks any changes to the armature, rails or input power could be judged for improvement in critical performance characteristics.

3.3.4 MCL13 - 12 kV Ripple Pulse; Laminated Armature

In previous work¹⁾ a monolithic armature was replaced by a stack of thin plate armatures cut to the same dimensions as the monolithic armature. In theory, the separate pieces of the armature act as individual contacts and can function better if violent interface events, such as gouging, occur. To test this hypothesis, two of the existing armatures were cut into slabs and machined to a thickness of 0.253". A 0.200" diameter hole was drilled in the forward section of each slab to accept a steel alignment pin. Kapton tape was applied to both sides of each slab to provide some electrical insulation. The individual slabs were fitted into a polycarbonate fore body and a 1.53" long steel pin inserted to stabilize the armature in the event of uneven current flow in the laminates. The assembled package mass increased by only six grams from the previous test. The package was loaded in the barrel and the power supply set to exactly the same parameters as the previous test. The data and railgun performance from shot MCL13 were, in many ways, identical to test MCL12 as seen by the shot data in Figure 3-7. The notable exception being the length of time that the muzzle voltage remained at a low level, approximately 370 μ s longer. The muzzle voltage trace in Figure 3-7 shows that transition did not occur until 2.7 ms when the velocity was estimated at 1.6 km/s.

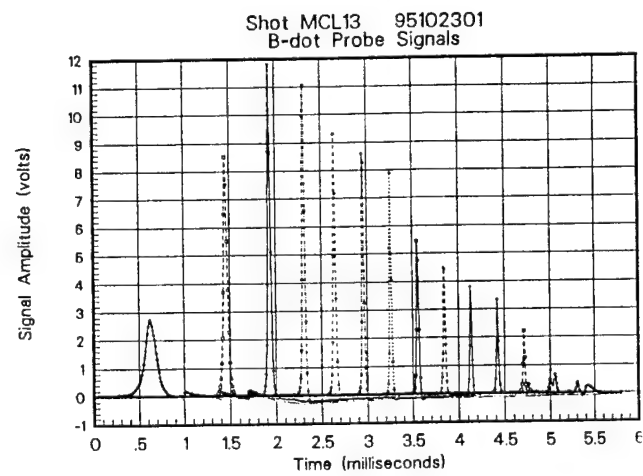
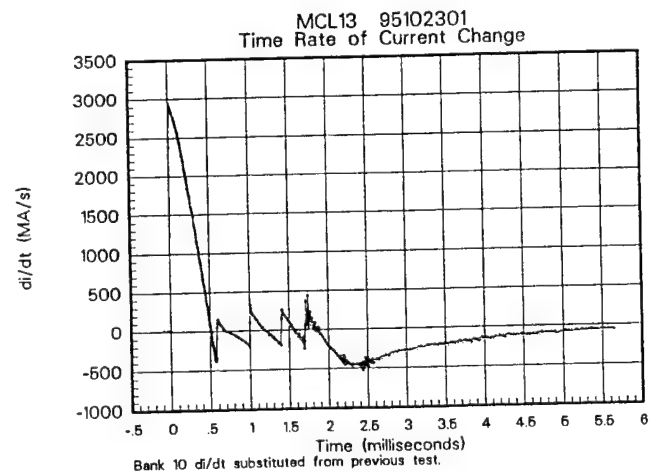
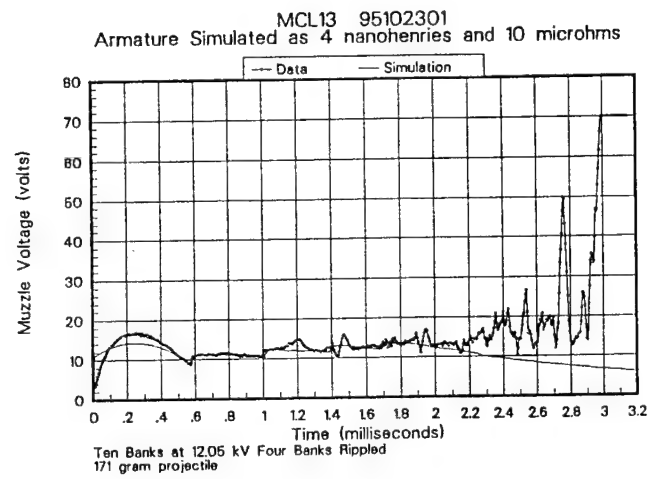
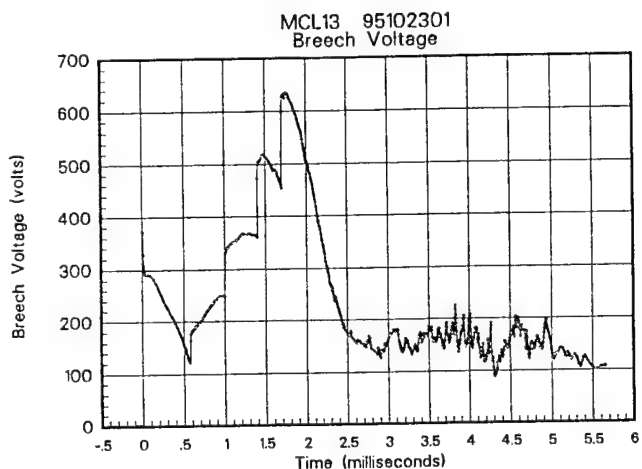
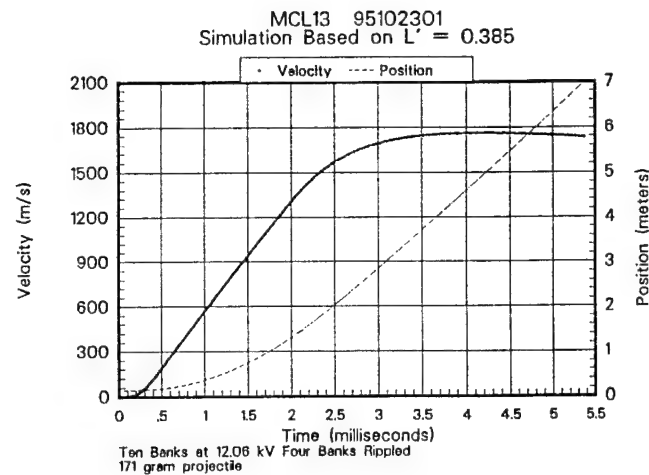
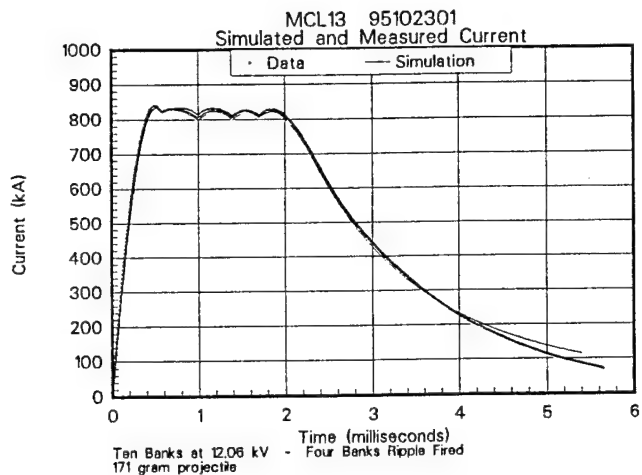


Figure 3-7 Shot Data for Test MCL13

The launch package reached a velocity of 1.8 km/s before exit, developing a quarter of a megajoule of kinetic energy. Only small pieces of the launch package were recovered from the soft catch system. The last two B-dot probe traces show small, multiple peaks raising the possibility that the projectile may have broken up in-bore.

Post shot inspection of the rails showed more gouges than the previous test but clearly a greater travel before transition. Wiping the soot from the muzzle end of the rails showed arc tracks with the same width as the laminates indicating that separate hybrid armatures may have formed from the individual laminates.

3.3.5 MCL14 - 12 kV Ripple Pulse; Grooved Faced Armature

It has been postulated that transverse grooves in a sliding contact could arrest gouge formation. To test this assumption 0.020" deep, "vee" grooves were cut into the faces the armature for Test MCL14. Three transverse grooves were cut at distances of 0.2, 0.5, and 0.8 inches from the leading edge of the contact face. Four axial grooves were also cut along the entire contact face with a spacing of 0.3". The armature was fitted to a polycarbonate fore body, loaded and fired with conditions identical to the two previous tests. Again, nearly identical power supply and railgun performance was observed as evidenced by the test data given in Figure 3-8. The armature behavior more nearly matched the solid, plain faced armature than the laminated armature. Contact transition occurred at 2.4 ms when the velocity was 1.54 km/s, the same as shot MCL12. Gouges were noted in the same general area on the rails although there were slightly fewer than MCL12 and considerably less than MCL13. Although badly damaged, 68 grams of the original 95 gram armature was recovered from the soft catch system.

The aluminum deposition on the rails began as individual stripes with a gap between the stripes equal to the width of the axial grooves. Further into the bore the gaps narrowed as though the armature was wearing away and the surface was approaching the bottoms of the "vee" grooves.

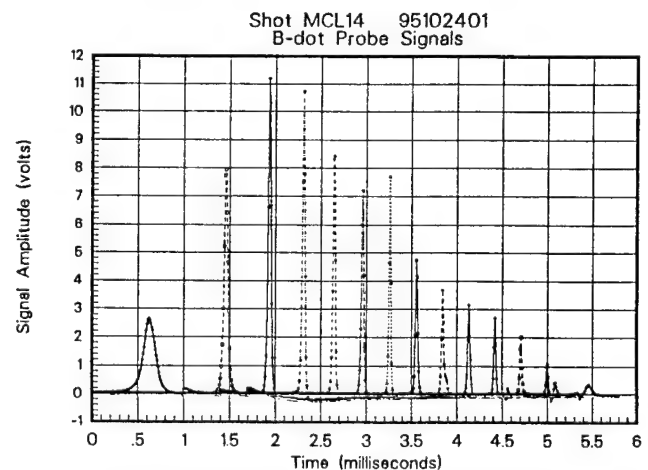
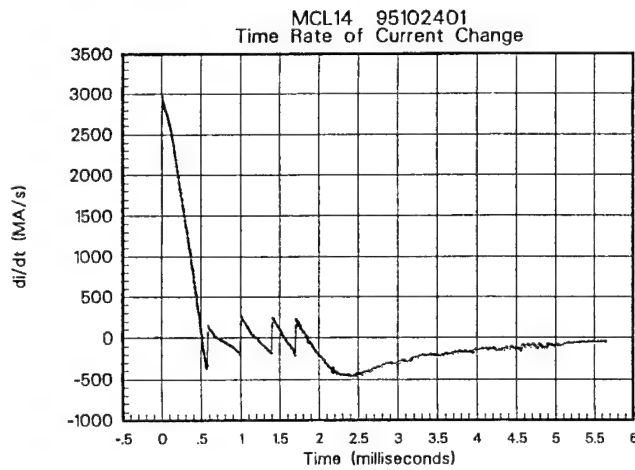
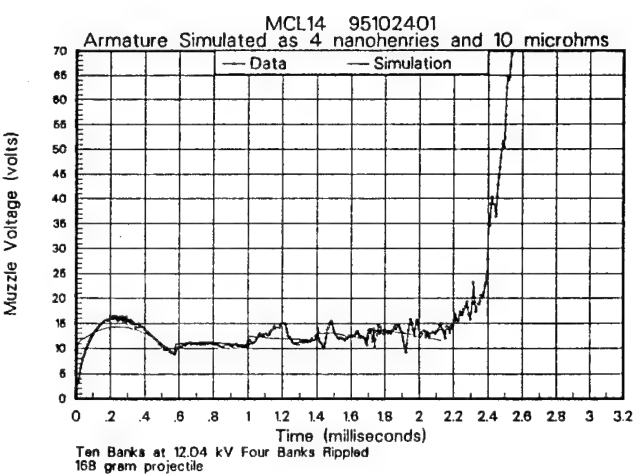
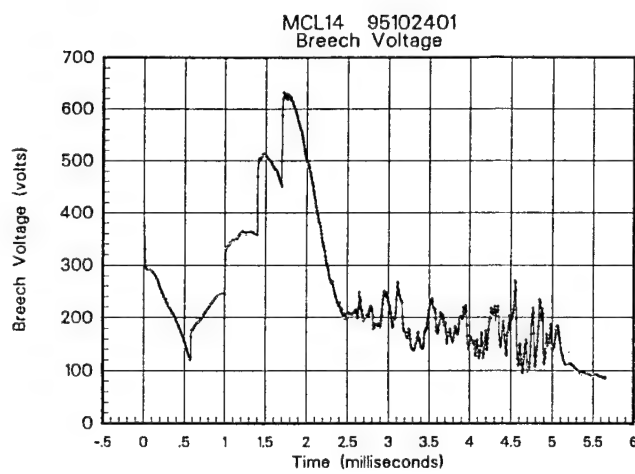
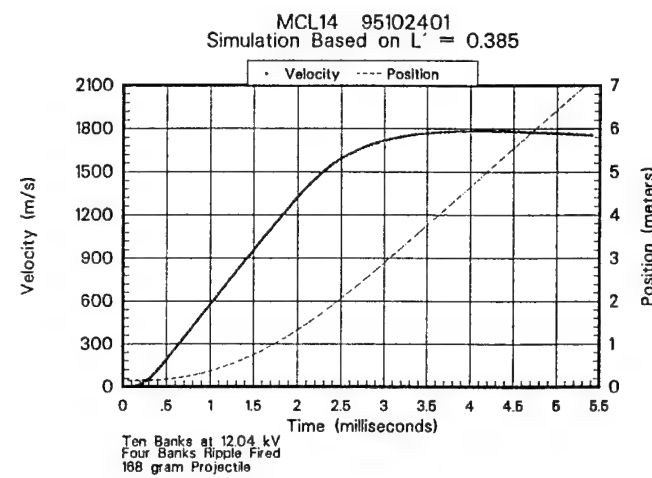
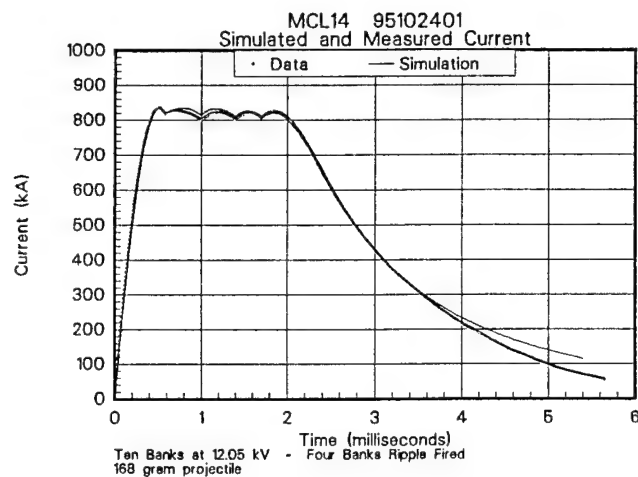


Figure 3-8 Shot Data for Test MCL14

This observation suggests the possibility of using axial grooves as a diagnostic technique to monitor contact erosion/abrasion.

3.3.6 MCL15 - 14 kV Ripple Pulse; Laminated Armature

Discussions with the entire test crew during the course of the last three tests led to the conclusion the final shot in the check-out test series should be a higher energy test using the best performing armature configuration from all of the previous shots. The laminated configuration used in Test MCL13 had shown the highest velocity and most travel before transition so it was selected for test MCL15. A second laminated armature was fabricated similar to the MCL13 armature but with a larger, 3/16 inch diameter steel pin. The 0.253" thick laminates were slightly chamfered on the edges of the contact faces to produce an effect similar to the transverse grooves. Again, Kapton tape was applied to both sides of the laminates for insulation.

Simulations showed that the current pulse would have to be compressed slightly to achieve a flat top when the capacitor charge voltage was increased from 12 to 14 kV. Delay times of 563, 950, 1288, and 1540 microseconds were assigned to the last four modules for the test. The launch packages were assembled and loaded as before. The modules were charged and fired at 14 kV.

The result was a projectile velocity of over 2.2 km/s with more than 0.4 megajoules of kinetic energy. The higher velocity reduced in-bore time to just over 4.4 ms. Peak current was very close to 1 MA as shown by the current trace in the upper left of Figure 3-9. The armature did not transition until 2.235 ms. It achieved an action of 2.2×10^9 A²s, 70% of the design goal. The velocity at transition was 1.97 km/s. The muzzle voltage briefly recovered to a low level before completely losing contact at 2.4 ms. The combination of high current and velocity resulted in over 900 volts on the breech and B-dot probe signals that approached 20 volts.

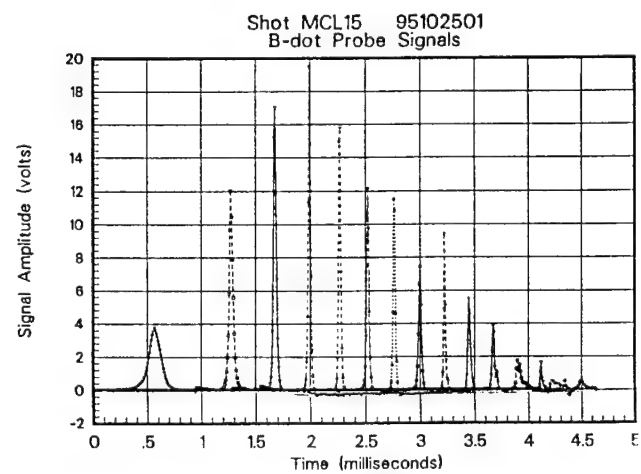
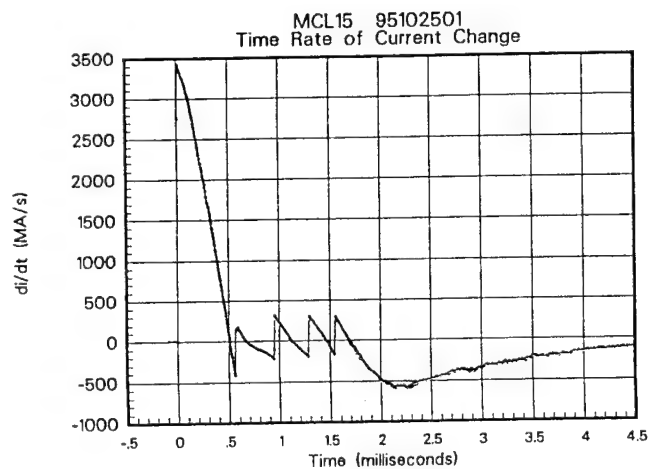
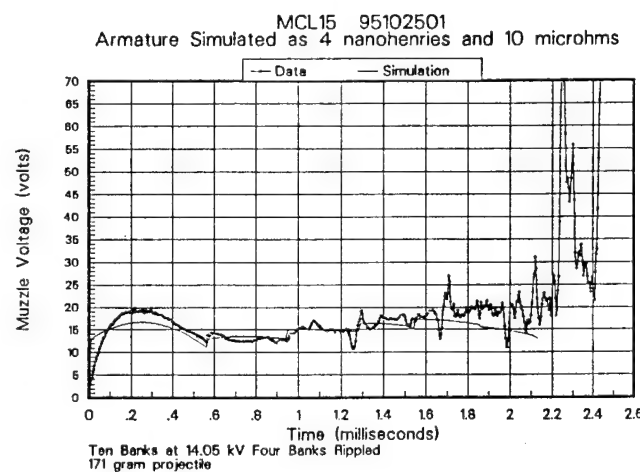
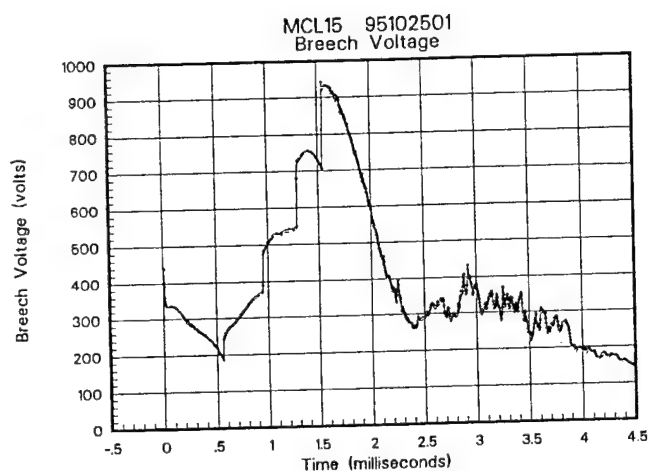
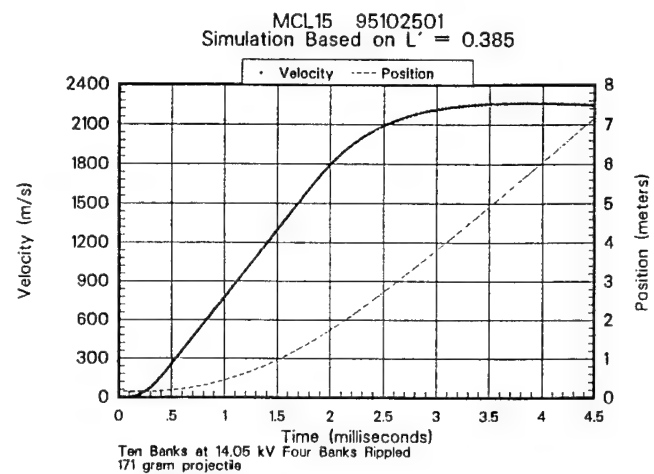
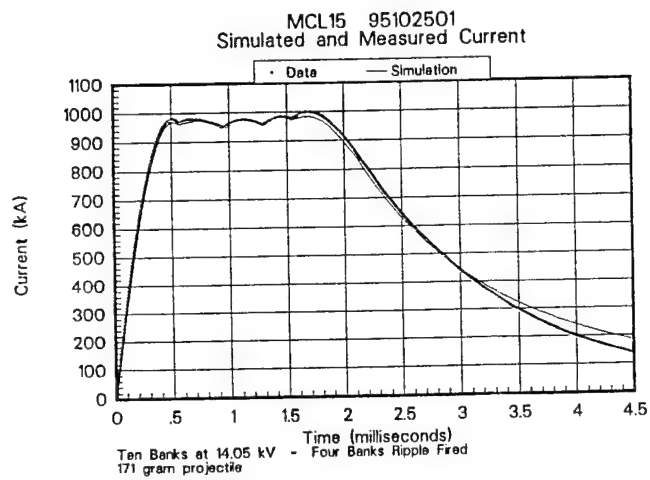


Figure 3-9 Shot Data for Test MCL15

Post shot inspection of the rails showed far more gouges than on any previous test. The onset of gouging did not occur until the velocity was 1.46 km/s. Location of most of the gouges was concentrated in the same general area of the barrel, from 1 to 3 meters from the breech with a few gouges beyond 3 meters.

4.0 Findings and Results

The original intent of this work was to characterize the performance of the MCL and provide a baseline set of armature performance data for future basic research efforts in armature-rail interactions. Essential to these future studies will be a power supply that is both reliable and predictable. The relative ease of operation and of matching simple, lumped parameter simulation codes with the observed currents in the testing reported here suggests both requirements are fully achieved. In terms of railgun performance, a critical parameter is the inductance gradient of the barrel. Substantial data now exists for both the electrical and mechanical behavior of the MCL in that regard. The armature performance data reported here is somewhat limited but it does provide a basis set in two areas, rail gouging and contact transitions.

4.1 Inductance Gradient

The static electrical testing indicated that the inductance gradient of the MCL was on the order of 0.48 microhenries per meter but the actual acceleration observed in the test firings did not support this finding. There are several ways to estimate the ability of the MCL to convert current to accelerating force. In this study the inductance gradient in a lumped parameter simulation code was adjusted until the arrival time at the tenth B-dot probe was matched (within 10 μ s) for shots MCL10 through MCL15. The tenth B-dot probe was selected for this analysis because it showed a noise free waveform in all tests and because most of the acceleration was complete before reaching the 4.83 meter location in the barrel. The simulation code includes a constant 1650 Newton (370 pounds) frictional drag force and a shock drag term that accounts for compressing and expelling the air in the bore as the projectile is accelerated. It simulates the discharge of each of the power supply modules to calculate a driving current. The inductance gradient and the square of the current are used to compute an accelerating force. The

equations of motion for the projectile are solved at each time step during the electrical discharge. The results given in Table 4-1 were obtained by performing multiple simulation runs with different inductance gradients and selecting the result that best matched the data. The findings indicate that the inductance gradient is well below 0.48, the average being 0.379 microhenries per meter. The "observed" inductance gradients tend to increase slightly with increasing shot energy. Also, the two tests with laminated armatures show the best inductance gradients.

Table 4-1 Inductance Gradient Needed to Match Simulations with Shot Data

Shot Number	Inductance Gradient ($\mu\text{H}/\text{m}$)	B-dot #10 Time (ms) [Experiment]	B-Dot #10 Time (ms) [Simulation]	Electrical Action ($\times 10^9 \text{ A}^2\text{s}$) [Experiment]	Electrical Action ($\times 10^9 \text{ A}^2\text{s}$) [Simulation]
MCL10	0.367	5.802	5.806	1.014	1.024
MCL11	0.371	4.502	4.506	1.327	1.340
MCL12	0.379	4.105	4.102	1.679	1.670
MCL13	0.387	4.137	4.138	1.699	1.672
MCL14	0.381	4.135	4.134	1.678	1.675
MCL15	0.388	3.455	3.456	2.177	2.123

The measured and simulated action integrals are also given in Table 4-1 as a cross check that the simulation code was correctly modeling the discharge of the capacitor modules. In general, the agreement is quite good.

As an aid to the post shot study of the rails, the measured muzzle voltage may be plotted as a function of the simulated in-bore position. Figure 4-1 shows the muzzle voltage, velocity and current versus the position of the armature in the barrel for three shots, MCL12, MCL13 and MCL14.

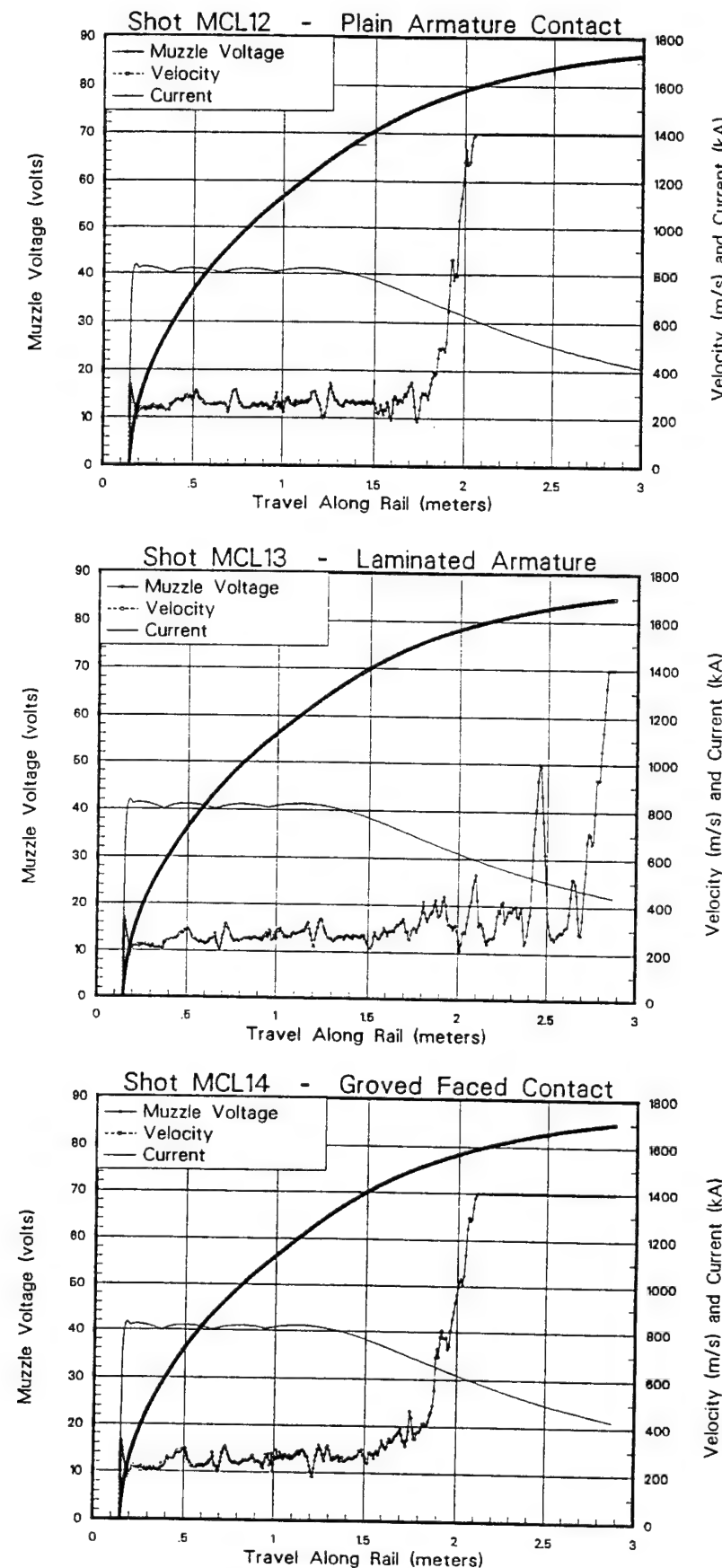


Figure 4-1 Muzzle Voltage versus In-Bore Armature Position for Three Shots

Data from the three tests given in Figure 4-1 were obtained from shots with identical electrical inputs and nearly equal launch package masses. Test MCL13 had a laminated armature and showed significantly more travel and velocity before transition occurred. All three muzzle voltage traces show some common features before contact transition. This is especially evident at the positions 0.73, 1.24 and 1.75 meters, the locations of B-dot probes #2, #3 and #4. These small amplitude oscillations are likely to be ferromagnetic effects because the probes are insulated from the laminated containment structure creating gaps in the reluctance path of the armature's magnetic field as the projectile passes the B-dot probes.

The laminated version of the check-out armature was selected for the highest energy shot, MCL15. The increased current gave rise to a higher transition velocity (nearly 2 km/s) when the armature had traveled just over two meters. Figure 4-2 shows the muzzle voltage, velocity and current for Test MCL15. Again, similar small features are evident in the muzzle voltage data before transition occurs.

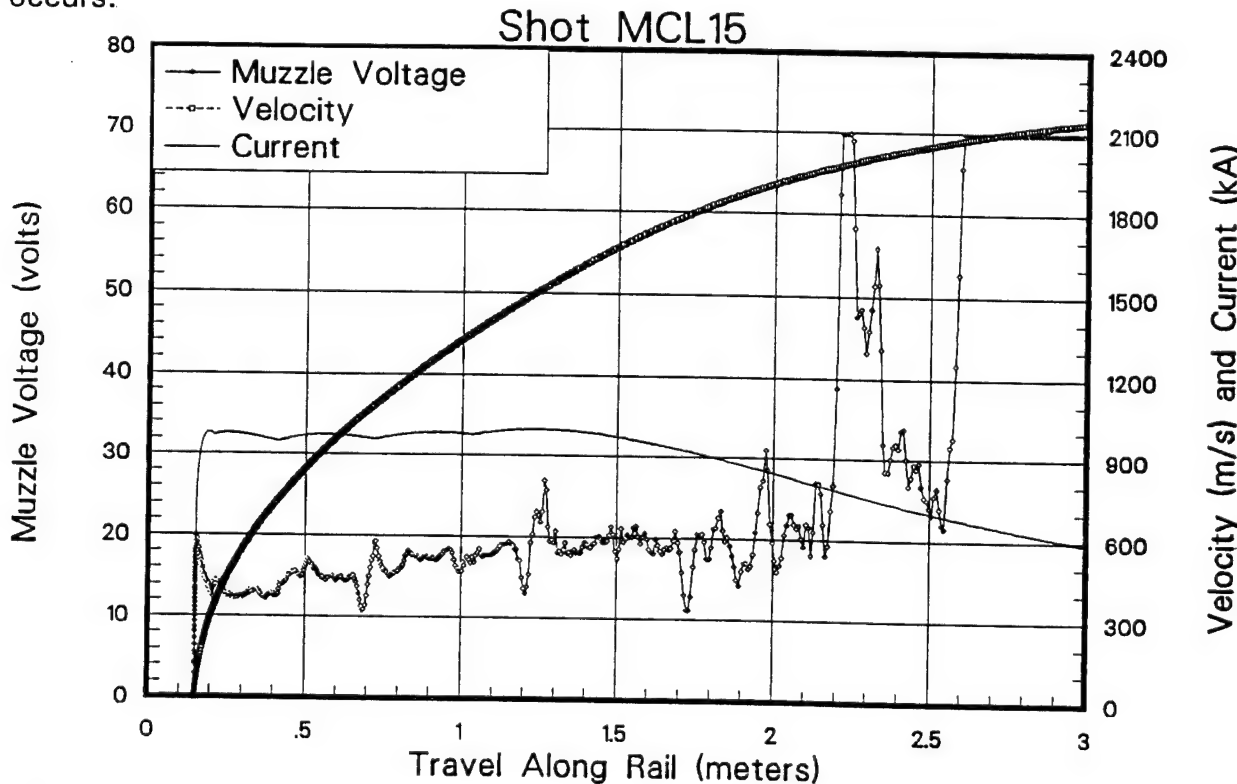


Figure 4-2 Muzzle Voltage, Velocity and Current versus Position for Test MCL15.

4.2 Rail Gouging

For tests MCL12 through MCL15 the in-bore velocity exceeded 1.7 km/s and considerable gouging was observed on the rails. To document the phenomena, the rails were replaced after each shot. This provided the opportunity to survey each rail and catalogue the gouges. Figure 4-3 shows the location and size of all of the significant gouges observed in the last four tests. No trend in gouge size versus location was noted. In all cases the gouges ceased after the armature had fully transitioned to a hybrid operation characterized by heavy soot, aluminum-copper alloy spots on the rails and arc tracks.

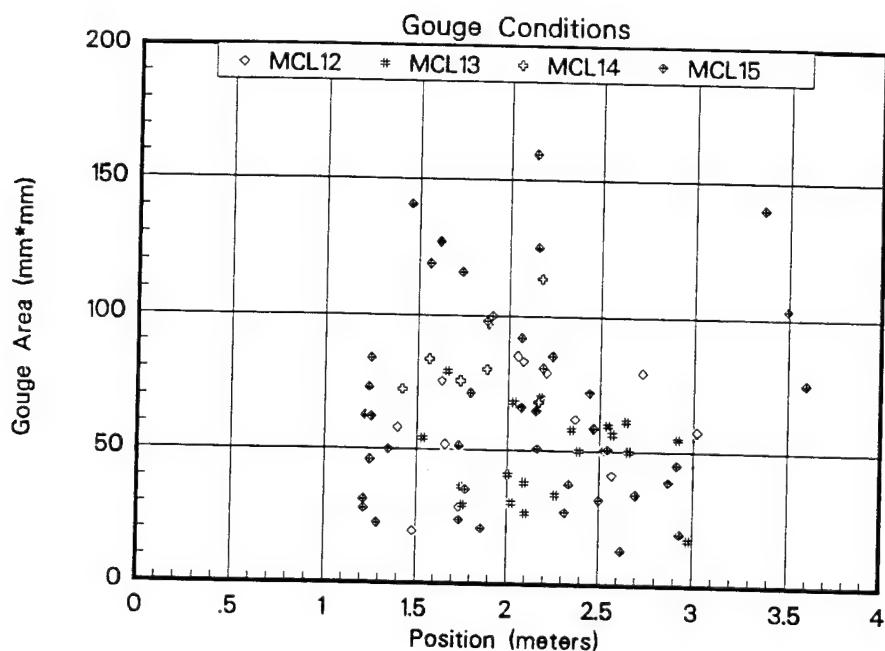


Figure 4-3 Location and Size of Rail Gouges

Most of the gouges were of the classic "tear drop" shape with slightly larger length (in the direction of projectile motion) than width. Figure 4-4 shows the length versus width for all of the gouges surveyed. As the symbols indicate the laminated armatures, MCL13 and MCL15 show more gouges than the monolithic armatures used in shots MCL12 and MCL14.

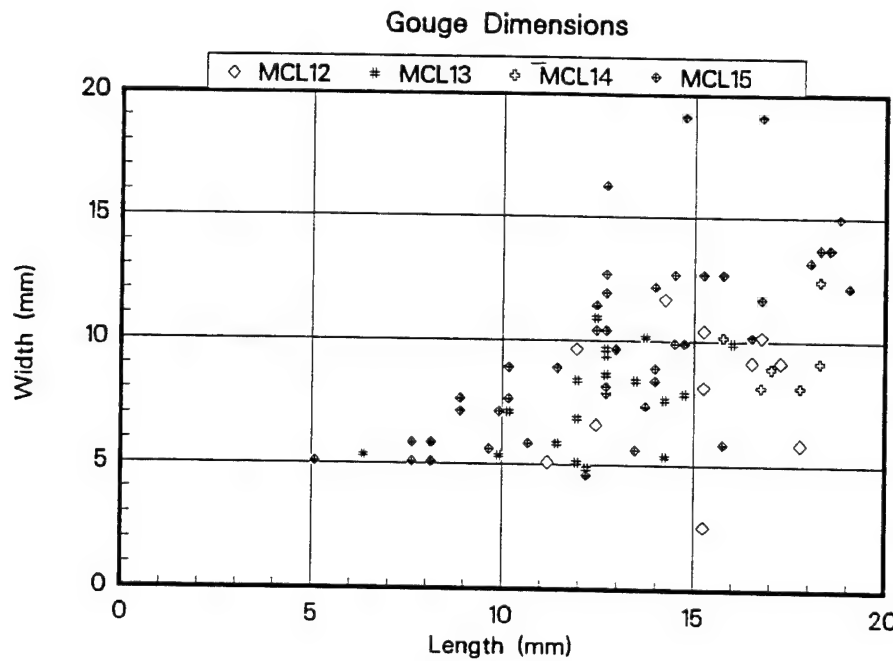


Figure 4-4 Gouge Length and Width

Given the apparent accuracy of the simulation codes discussed in the previous section, the gouge locations may be cross referenced to velocity and current in each test. The results are displayed in Figure 4-5 that shows both the current and velocity of the projectile at the location that each gouge occurred.

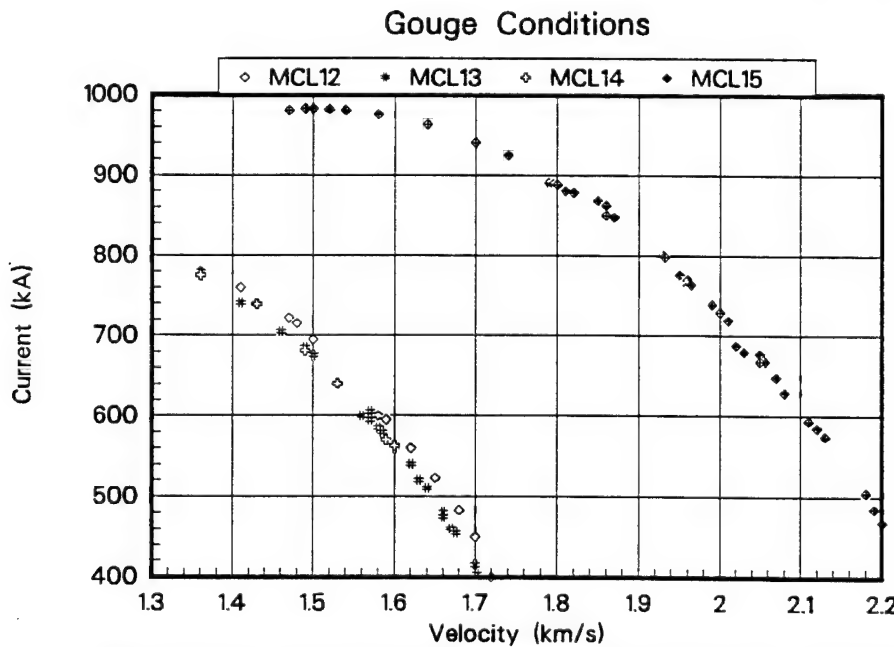


Figure 4-5 Velocity and Current at Each Gouge Location.

The lowest velocity that a gouge occurred was 1.35 km/s. As velocity increased, gouges continued to occur, apparently at random, until the armature had fully transitioned. The near overlap of the curves for shots MCL12-14 in Figure 4-5 is evidence of the precision of the total system in its ability to replicate test conditions on demand.

4.3 Contact Transition

All of the firings reported here included events that are referred to as contact transition. For this work transition is defined as an excursion of the muzzle voltage 15 volts above the running level. In tests MCL13 and MCL15 the voltage recovered briefly after transition but performance after the first transition is not considered here. Table 4-2 summarizes the characteristics of the transitions of all six live shots in the check-out test series. In general, the armatures performed better under higher loads. Specifically, each time the energy input to the gun was increased, the velocity at transition increased.

Table 4-2 Transition Conditions for Entire Shot Series

Shot	Electrical Action $10^9 \text{ A}^2\text{s}$	Transition Time (ms)	Velocity (Simulation) (km/s)	Current at Transition (kA)	Travel (m)	Magnetic Pressure (ksi)
MCL10	0.970	3.47	0.98	199	2.40	0.6
MCL11	1.194	2.31	1.28	396	1.74	2.7
MCL12	1.390	2.37	1.54	667	1.71	7.3
MCL13	1.525	2.74	1.64	517	2.28	4.5
MCL14	1.399	2.40	1.54	651	1.74	7.1
MCL15	1.835	2.235	1.97	781	2.05	10.1

"C" shaped armatures derive most of their contact force loading from the magnetic forces repelling the armature legs. As such, it is not surprising that

improved performance is achieved when a higher current is applied for a longer time. Figure 4-6 illustrates this point by graphing the electrical action incurred before transition versus the magnetic pressure that existed in the bore at the time of transition. The general trend is that under higher pressure the armature can withstand greater electrical loading before transition occurs.

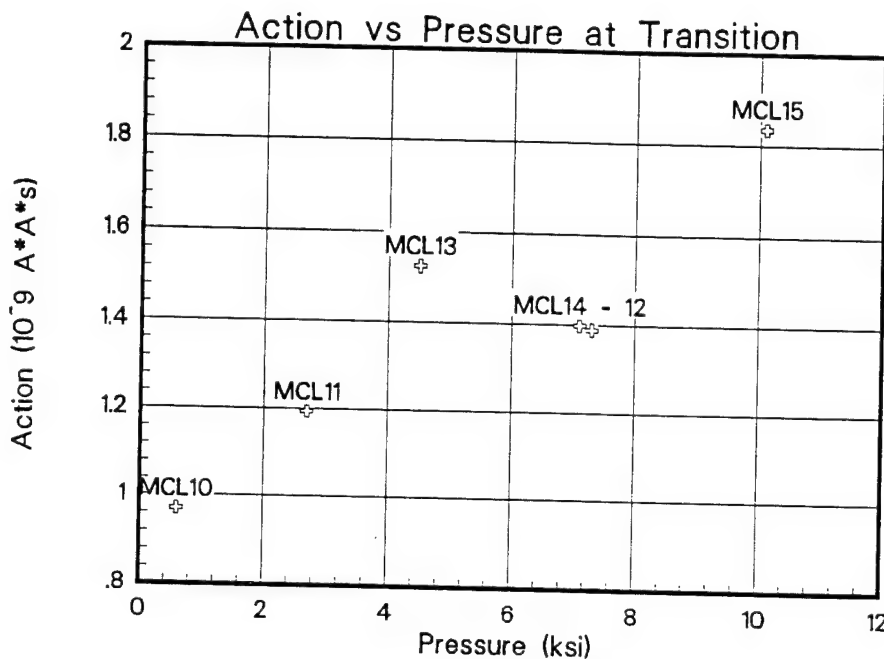


Figure 4-6 Electrical Action versus Magnetic Pressure at Transition

5.0 Conclusions

The relative ease of operating the IAT-HVL power supply, railgun and diagnostics in their check-out phase clearly shows their potential as a very good laboratory test bed for the study of armature behavior. In fact, the last three shots of this study were performed on successive days even with total disassembly of the barrel and replacement of the rails on each shot. The diagnostic array appears to be well suited to the study of armature contact function. The length of the MCL

ensures that these studies will have time scales appropriate to military applications.

The inductance gradient of the MCL was somewhat lower than expected. A gradient of $0.38 \mu\text{H/m}$ gave adequate simulation of the acceleration observed in the test firings. Static electrical tests, however, showed a higher inductance with a gradient of $0.48 \mu\text{H/m}$ giving a better match to the electrical data.

A simple, baseline armature was tested under a variety of load conditions. It showed more resistance to transition when operated in a laminated configuration with five separate pieces comprising the armature. As expected for "C" shaped armature designs, resistance to contact transition was also improved when the magnetic pressure was increased. Although exploration of armature behavior was limited in this work, a baseline has been established. The best shot demonstrated a velocity of 1.97 km/s before transition occurred. It is hoped that the baseline data established here will help to build a much more detailed study of armature contact behavior.

References

1. R. A. Marshall, "The OAT Armature/Rail Experiments," Institute for Advanced Technology Technical Report, IAT.R0072, June 1995
2. J. H. Price and H. D. Yun. Design and Testing of Integrated Metal Armature Sabots for Launch of Armor Penetrating Projectiles for Electric Guns," *IEEE Trans. on Magnetics*, Vol. 31, No. 1, pp.219-224, January 1995.
3. M. J. Matyac. F. Christopher, K. A. Jamison, C. Persad and R.A. Marshall, Railgun Performance Enhancement from Distribution of Energy Feeds," *IEEE Trans. on Magnetics*, Vol. 31, No. 1, pp.332-337, January 1995.

4. J. V. Parker, D. T. Berry, and P. T. Snowden, "A New Electromagnetic Launcher Research Facility at the Institute for Advanced Technology," European Electromagnetic Launcher Symposium, April 1995.

Acknowledgment

The author is grateful to the IAT-HVL for the opportunity to assist with their basic research efforts in the fundamental behavior of solid armatures in railguns. This work, in particular, was made possible by two prior efforts: a well crafted railgun procured by the IAT from IAP Research, Inc. Dayton, OH, and a power supply constructed by the HVL staff lead by Dr. Jerald Parker. Historically, both railgun and pulsed power facilities have required numerous "on-the-spot" modifications to complete a commissioning test series. In this case, neither required any significant changes.

The results documented here were obtained through a team effort for which the author is indebted to Dr. Jerald Parker, Dr. Scott Levinson, Mr. Paul Snowden, Mr. Harry Hart, and Mr. Ron Stearns. Their diligence and willingness to "get the job done" made these experiments possible.

This work was supported by the U.S. Army Research Laboratory (ARL) under contract number DAAA 21-93-C-0101.

Appendix A
MCL Check-Out Test Plan

MCL Check-Out Test Plan

Draft - 17 September 1995

The initial characterization of a launcher can provide very useful information to all subsequent R&D projects utilizing that equipment. Since power supplies and launchers are coupled, a well-documented set of experiments can be a significant benefit in the planning of future armature research topics. Given the significance of the task it is generally useful to plan the characterization tests for a new launcher even though such plans are seldom fully conducted in their original form. The basic design of the MCL follows a long line of launchers that have proven themselves in a wide variety of performance and utility. For that reason, a rather aggressive checkout procedure is recommended. What is proposed here are three static (locked armature) tests followed by a five shot test sequence that moves up slowly in peak current but very aggressively in armature velocity. The results from simulations of the proposed shots are outlined in the table below.

Proposed Characterization Shot Sequence

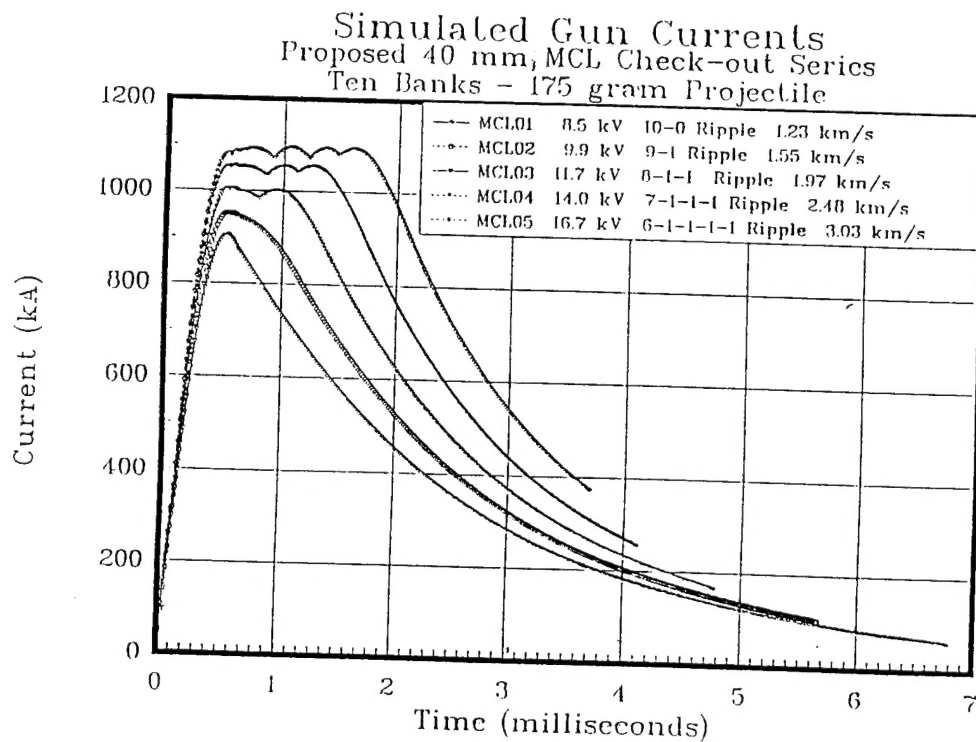
Simulations Based on 175 gram Projectile

Shot #	Charge Voltage (kV)	Peak Current (kA)	Exit Velocity (km/s)	Acceleration Time (ms)	Ripple Scheme	Kinetic Energy (kJ)	System Efficiency (%)
MCL01	8.5	900	1.23	6.72	10-0	130	8.1
MCL02	9.9	950	1.55	5.60	9-1	210	9.6
MCL03	11.7	1000	1.97	4.72	8-1-1	340	11.0
MCL04	14.0	1050	2.48	4.07	7-1-1-1	540	12.2
MCL05	16.7	1100	3.03	3.67	6-1-1-1-1	800	12.8

The static tests, one with the armature in the initial load point, one with the armature half way down the bore, and one with the armature locked in the muzzle are needed to refine the parameters used in the simulation code. A single bank charged to 8 kV will produce a current of about 100 kA if the output cables are shorted. The anticipated currents for the locked armature tests are 90, 82, and 80 kA, respectively. Accurate measurement of the time rate of change of current (approximately 300 MA/s) and the breech voltage will yield the gun inductance. The differences from these measurements can be used to derive the inductance gradient of the launcher. The accelerating force on the armature is expected to be less than 400 pounds so that it should not be too difficult to lock the armature in place. Measurements of the muzzle voltage and armature current can be used to estimate armature resistance and inductance. These values are essential for predicting muzzle voltage in an actual shot. Differences in predicted and observed muzzle voltage are the corner stone of the study of armature/rail interface phenomena.

When the locked armature testing is complete, the refined launcher parameters, armature circuit characteristics, the final design mass of the launch package, and any required modifications to the power supply parameters will be input to the simulations and new runs completed. These new simulation runs will be used as a benchmark to monitor the performance of the launcher in the initial checkout test series. An example of the simulation output that will be used to monitor the shot data is given in the attached figure that shows railgun current versus time for the proposed test sequence. Again, the philosophy of the test plan is to move up gradually in current (armature stress) while moving up aggressively in the exit velocity of the launch package.. This is rather easily accomplished by adjusting the firing times of the power supply to broaden the current pulsed and bank energy is increased.

The completed data set from the static tests and the five shot test sequence will provide an excellent predictive tools for planning armature experiments. The results should be well documented in a "users guide" to assist future researchers.



Distribution List

Commander
U.S. Army Armament Research,
Development and Engineering Center
Attn: AMSTA-AR-FS (Ted Gora) Bldg. 94
Picatinny Arsenal, NJ 07806-5000

Commander
U.S. Army Armament Research,
Development and Engineering Center
Attn: SMCAR-FSE (Dennis Ladd) Bldg. 382
Picatinny Arsenal, NJ 07806-5000

Commander
U.S. Army Armament Research,
Development and Engineering Center
Attn: AMSTA-AR-CCL (Bob Schlenner)
Bldg. 65N
Picatinny Arsenal, NJ 07806-5000

Dr. Ingo W. May
Office of the Director
Army Research Laboratory
ATTN: AMSRL -WT
Army Research Laboratory
APG, MD 20115-5066

Mr. Albert Horst
Chief, Propulsion and Flight Division
Army Research Laboratory
ATTN: AMSRL -WT-P
Army Research Laboratory
APG, MD 20115-5066

Director
U.S. Army Research Laboratory
Attn: AMSRL-WT-PB (Edward Schmidt)
APG, MD 21005-5066

Alex Zielinski
U.S. Army Research Laboratory
AMSRSL-WT-PB, B390, RM 212
APG, MD 21005-5066

Office of the Assistant Secretary
of the Army (RDA)
Attn: Dr. Richard Chait
Deputy Asst. Secretary of the
Army for Research & Technology
The Pentagon, Room 3E374
Washington, DC 20310-0103

Dr. John P. Barber
IAP Research, Incorporated
2763 Culver Avenue
Dayton, OH 45429-3723

Brad Goodell
United Defense LP
Mailstop M401
4800 East River Road
Minneapolis, MN 55421-1498

George Chryssomalis
SAIC
3800 W. 80th St., Suite 1090
Bloomington, MN 55431

Robert Taylor
Lockheed Martin Vought Systems
P.O. Box 650003
Dallas, TX 75265-0003

Raymond C. Zowarka
Center for Electromechanics
The University of Texas at Austin
Pickle Research Campus
EME 13, C R 7000
Austin, TX 78712

Dan Dakin
Science Applications International Corp.
2200 Powell St., Suite 1090
Emeryville, CA 94608

Administrator
Defense Technical Information Center
Attn: DTIC-DDA
Cameron Station
Alexandria, VA 22304-6145

Dr. Robert Guenther
Army Research Office
P.O. Box 12211
Research Triangle Park, NC 27709-2211

Russ Klug
Wright Laboratories
WL/ MNMW
Eglin AFB, FL 32542

Mr. Dennis Hildenbrand
PKD New Jersey
520 Speedwell Ave., Suite 108
Morris Plains, NJ 07950

Dr. Keith A. Jamison
Science Applications International Corp.
1247-B N. Eglin Parkway
P. O. Box 126
Shalimar, FL 32579